INCREASING THE DRAWBAR PULL OF BAŞAK TRACTOR FOR ARID LAND CULTIVATION : A THEORETICAL INVESTIGATION OF IRON WHEEL

A Master's Thesis

Presented by

ABDILKADIR MOHAMMED MUSA

to

the Graduate School of Natural and Applied Sciences

of Middle East Technical University

in Partial Fullfillment for the Degree of

MASTER OF SCIENCE

in

MECHANICAL ENGINEERING

MIDDLE EAST TECHNICAL UNIVERSITY

ANKARA

February, 1994

Approval of the Graduate School of Natural and Applied Sciences.

Prof. Dr. İsmail TOSUN
Director

I certify that this thesis satisfies all the requirements as a thesis for the degree of Master of Science in Science Engineering.

Prof.Dr. Rüknettin OSKAY
Chairman of the Department

We certify that we have read this thesis and that in our opinion it is fully adequate, in scope and quality, as a thesis for the degree of Master of Science in Mechanical Engineering.

Prof.Dr. Alp ESİN
Supervisor

Examining Committe in Charge :

Prof.Dr. Y. Samim ÜNLÜSOY (Chairman)

Prof.Dr. Alp ESİN (Supervisor)

Prof.Dr. A.Erman TEKKAYA

Prof.Dr. Demir BAYKA

Assoc.Prof.Dr. Ayhan İNAL (CE)

ABSTRACT

INCREASING THE DRAWBAR PULL OF BAŞAK TRACTOR FOR ARID LAND CULTIVATION : A THEORETICAL INVESTIGATION OF IRON WHEEL

MOHAMMED, Abdılkadir

M.S. in Mechanical Engineering

Supervisor : Prof.Dr. Alp ESİN

February 1994, 149 pages

It has long been recognised that in order to increase the agricultural production in developing countries and especially in Kenya, the agricultural activity need to be mechanized. In the last three decades numerous attempts have been made to develop a feasible mechanization tool for tropical arid and semi-arid regions but unfortunately none of this have achieved any mentionable success.

The aim of this study was to develop a feasible mechanization tool for tropical arid and semi-arid regions. Different models of small tractors were studied for their suitability for cultivation in the above mentioned agricultural region and small 4-wheel ride-on tractor

model was found as the best solution. Başak-17 tractor was taken to represent small 4-wheel ride-on tractor model and to improve the tractor's operational performance, the use of Iron-Wheel was proposed.

Passive earth pressure theory was used to model the Iron-Wheel lug-soil interaction and the model was made to take into account the effect of soil's compressibility. Equations for predicting the tractor's operational performance were derived and a rational design procedure developed.

The theoretically predicted results show that the drawbar pull of Başak-17 is improved by about 300 %, which is well above that required for cultivation of arid and semi-arid regions.

The results obtained from this study are very encouraging as a small tractor of Başak-17 size fitted with Iron-Wheels could provide a solution to mechanization problem of arid and semi arid agriculture.

Keywords : Small farm Mechanization, Soil-lug modelling, Iron-Wheel, Drawbar pull.

Science Code : 625. 01. 07

ÖZ

ÇORAK ARAZİNİN İŞLENEBİLMESİ İÇİN BAŞAK TRAKTÖRÜNÜN ÇEKİ KUVVETİNİN ARTIRILMASI : ÇELİK TEKERLEK ÜZERİNE TEORİK ÇALIŞMA

MOHAMMED, Abdılkadir
Yüksek Lisans Tezi,
Makina Anabilim Dalı
Tez Yöneticisi : Prof. Dr. Alp ESİN
Şubat, 1994, 149 sayfa

Gelişmekte olan ülkelerde, özellikle Kenya'da tarımsal verimi artırmak için tarımın mekanizasyonu uzun süredir üzerinde durulan bir konudur. Son otuz yıldır tropik ve yarı-çorak bölgelerde kullanılabilir mekanizasyon araçları geliştirilmesi yolundaki çabalarda kayda değer başarı kazanılamamıştır.

Bu çalışmanın amacı, tropik ve yarı-çorak bölgelerde kullanılabilir mekanizasyon aracı geliştirmektir. Değişik küçük traktör seçenekleri üzerinde durulmuş ve üzerinde sürücüsü olan dört tekerlekli traktör modelinin en geçerli seçenek olduğu görülmüştür. Başak-17 traktörü bu grubun temsilcisi olarak ele alınmış ve performansını geliştirmek amacıyla çelik tekerlek kullanılması

incelenmiştir.

Toprağın sıkıştırılabilirliğini de gözönünde tutarak, pasif zemin basıncı teorisi ile çelik tekerlek modellemesi yapılmış, böyle bir tekerleğin performansı hesaplanmış ve akılcı bir tasarım yöntemi geliştirilmiştir.

Teorik sonuçları, Başak-17 traktörünün çeki kuvvetinin, çorak ve yarı-çorak arazinin sürülmesi için gerekenin üstünde, % 300 artabileceği sonucunu vermiştir.

Çalışma sonuçları çok olumlu olup, Başak-17 emsali küçük traktörlere çelik tekerlek uygulanması ile çorak ve yarı-çorak bölgelerin tarımsal mekanizasyonuna çözüm getirebileceği ortaya konmuştur.

Anahtar Sözcükler : Küçük çiftliklerin mekanizasyonu, toprak-kaz ayağı modellemesi, Çelik tekerlek, Çeki kuvveti.

Bilim Kodu : 625. 01. 07

ACKNOWLEDGEMENT

The author wishes to express his deepest gratitude to his supervisor Prof.Dr. Alp ESİN, for his patience, guidance and encouragement through out the study period.

The author also wishes to thank Prof.Dr. Samim ÜNLÜSOY for providing a conducive working environment.

Special thanks go to Mrs Özden ERDEMLİ for undertaking the monumental task of typing this work under the most trying conditions.

TABLE OF CONTENTS

LIST OF FIGURES

LIST OF TABLES

CHAPTER I
INTRODUCTION

1.1 General

In most developing countries and especially in Kenya, agricultural sector is the most important as it employs 85% of total rural labour force and generates 60 % of the foreign exchange. With a rapid increase in population of about 4 % per year, there's urgent need to enhance both labour and land productivity.

In Kenya, out of 1.240.000 ha cultivated land about 1,000,000 ha is cultivated manually, 200.000 ha by animal drawn implements and only 40, 000 ha by mechanical power[1]. Africa, in general, fares much less favourably as compared to other regions in the world in utilizing animal power and mechanical power as can be seen from Figure1.1 [2].

Research has shown that hand digging consumes human energy at the rate of 12 Kcal/mn. This would amount to about 750 Kcal/h[1]. Since human energy available for work is only about 1500 Kcal/day then an adult can sustain hand cultivation for only 2 hours a day in tropical climate. A typical rate of cultivation is about 0.5 ha per season and this is consistent for most of Africa. Due to the

inability of the farmer to cultivate more than 1.5 ha of land per season; (based on three adults per homestead) the remaining part of the land is left to fallow. As table 1 shows only 37.1% of the land owned as farm land in Kenya is under cultivation [1].

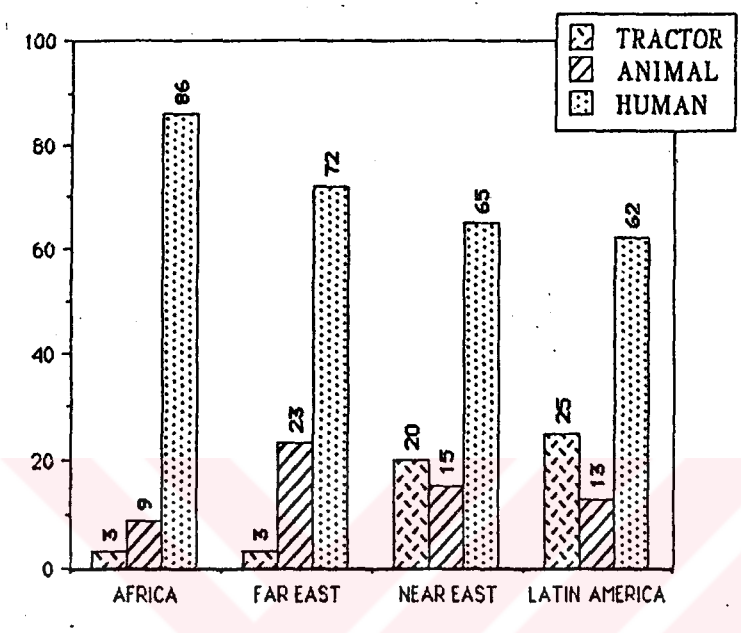

Figure 1.1 Percentage of Power Input in Agricultural Operations. [2]

Table 1.1 Land utilization by provinces (small farms only) (X 1000 ha). [1].

	Provinces						Total
	Central	Coast	Eastern	Nyanza	Rift valley	Western	
area of holding[1]	880.1	116.0	769.3	744.9	267.8	630.2	3458.3
area under cultivation[2]	291.1	111.6	434.0	232.4	74.3	132.9	1281.9
additional area planted in 1975	224.8	65.0	354.8	264.1	68.9	247.5	1225.0

[1] Excludes pastures and large farms.
[2] Includes permanent crops but excludes fallow and pasture.

This unexploited land does not in anyway contribute to the income of the farmer and the national food production, and thus any enhancement of labour and land productivity should be made by first increasing the power at the disposal of the farmer.

Increasing the power at the disposal of the farmer can be done by either adopting to a greater extent animal or mechanical power. Animal power could be used in high and medium potential areas where farmers have a tradition of mixed farming and where the cost of keeping a pair of oxen is not high. In areas where there's no tradition of animal husbandry, coupled with tse-tse fly problem, attempts to introduce animal drawn implements in this areas have invariably failed [3]. In semi-arid region, a pair of draught animal cannot develop the required drawbar pull of 5KN for primary cultivation[1] and farmers are forced to wait for the onset of rain before embarking on land cultivation; thereby losing valuable moisture which leads to low yield [4]. Therefore areas where animal drawn implement can be introduced are small as compared to otherwise, Table1.2 [1]. The low potential or semi-arid region comprises 81% of Kenya's agricultural land, thus tractors should be introduced in greater number in order for any worthy mechanization of agriculture in Kenya is to occur.

It can be readily followed from Table1.3 that the increase in the number of tractors per 1000 ha of land not only increases the acreage of farmland that can be cultivated per unit time, but also the yield/ha [2], areas where the number of tractors per 1000 ha is high, the yields in tonnes/hectare of various crop are also high.

Table 1.2 Categories of agricultural land according to rainfall (x1000 ha). [1].

Province	High potential (857.0mm)	Medium potential (735-857.0mm)	Low potential (612mm or less)	Total	All other land	Total land area
Central	909	15	41	956	352	1318
Coast	373	796	5663	6832	1472	8304
Eastern	503	2189	11453	14145	1431	15576
Nairobi area	16	_	38	54	14	68
North eastern	_	_	12690	12690	_	12690
Nyanza	1218	34	_	1252	_	1252
Rift valley	3025	123	12220	15368	1515	16883
Western	741	_	_	741	82	823
grand total	6785	3157	42105	52047	4867	56914

Table 1.3 Degree of Mechanization and crop yield/hectare. [2].

	Number of tractors per 1000 ha	wheat tonne/ha	rice tonne/ha
ECC	61.0	4.4	5.4
The Netherlands	90.0	6.7	-
USA	23.0	2.3	5.5
Japan	390	3.1	5.6
Developing countries			
Far east	2.2	1.6	2.3
Near East	3.5	1.5	4.2
Africa	1.2	1.0	1.4
Latin America	5.0	1.5	1.9

Most tractors and agricultural machinery now in operation in Kenyan farms have power output above 50 Hp. These tractors can only be used efficiently on large farms which form a small percentage of the total cultivated land. Any attempt to use these

tractors and agricultural machinery on a typical small scale farm results in a failure as the initial cost is high and the annual number of hours of tractor utilization is low; and thus the cost-benefit balance is always negative.

As an example consider a farmer who owns less than five hectares; they constitute about 75 % of farm holders as shown in Table 1.4 [2] Supposing that such a farmer acquires a 64Hp tractor with which it takes 2.2 hours per hectare for primary cultivation, thus primary cultivation takes about 11 hours [4]. Clearly, the total utilization of the tractor time would be less than 28 hours per year as a result of which the tractor either has to be hired out or lie idle the rest of the time. Therefore a new strategy should be adopted and tractors developed for mechanization in Kenya or any other tropical countries should have the following characteristics. These characteristics are treated under the following subheadings for the sake of clarity.

Table 1.4 Percentage Distribution of Small-holding by Site and Province (except the large farms and pastoral lands). [1].

acreage (ha)	province(%)						
	Central	Coast	Eastern	Nyanza	Rift valley	western	total
below 0.5	6.74	20.37	9.55	15.72	22.99	21.53	13.91
1-2	10.50	18.46	17.36	28.18	12.11	17.67	17.92
2-3	36.96	22.52	33.39	22.03	17.59	17.27	26.99
3-4	11.86	7.68	8.57	6.79	10.11	8.60	8.89
4-5	5.92	8.15	9.63	8.13	5.72	4.36	7.22
5-8	7.63	5.87	5.43	4.09	6.87	10.22	6.50
8 and more	3.92	5.53	1.22	1.83	9.83	5.68	3.47
number of holdings	329530	69861	353431	386431	89823	254618	1483422

1.2 Appropriately Powered

By the term appropriately powered it is meant that the tractor's engine power should be such as to match the farm's power requirement so as to avoid excess tractor idle-time, which is a common phenomenon in small farms that have bought commercially available medium powered tractors. The main reason for failure of mechanization policies in the tropical countries is the inherent power mismatch between the commercially available medium powered tractors and the small-farm's power requirements.

1.3 Enough Drawbar Pull

A requirement which is contradictory to the above requirement but which forms the engineering challenge of the problem at hand is the high drawbar pull. Drawbar pull is a term used for pull exerted by the tractor on an agricultural implement or trailer. Most of the small-tractors designed for mechanization of small-scale farms cannot develop enough drawbar pull required for primary cultivation. Crossley [4] reports that the draught force required to operate a single implement (chisel plough or mouldboard plough) at a depth of 150 mm in dry season is in the range between 3-5 KN. As it would later be seen most of small tractors designed for small-scale farms cannot produce the required drawbar pull. This has made it quite uneconomical for farmers to purchase these tractors as the work-rate and quality of cultivation have been unacceptably low.

1.4 Low Cost

The tractor's small size should automatically make it cheaper and thus affordable to small scale farmers but care has to be taken in not making it very cheap and crude and thus reduce the social acceptability which is a peculiar but important constraint.

1.5 Other Characteristics

As the operating and climatic condition are harsh in tropical countries, the tractors should be rugged and sturdy. The sliding and rotating parts of the tractor should be protected from abrasive dust particles which are quite common during the dry seasons. The tractor should have high clearance so as to avoid getting grounded in ridges or stuck in furrows. In addition to the above mentioned requirements the tractor should have all other charactersitcs of a well designed machine.

1.6 Estimates of Small Tractor Demands

For farms producing cereals, a small-tractor would be used most efficiently and economically in farms which are 5 hectares and above. As Table 1.4 shows, these farms make 9.97% of the total farms in Kenya's small holder sector, or about 150,000 farms.

Going back to Table1.1 it can be seen that about 63 % of Kenyan farm land is uncultivated. Assuming that a proportional

amount of land is not cultivated in farms with sizes above 5 hectares as well and that for the cultivated areas, due to lack of mechanization and other yield increasing inputs like fertilizers and pesticides, the yield is only 1 tonne/ha, equal to Africa's average as shown in Table 1.3. Acquiring a small tractor would allow the farmer to achieve an almost 100% land utilization and increase yield to 2.3 tonnes/ha (lowest among countries with good mechanization. Table 1.3). The price of cereal being about 200$/tonnes in international markets, the increase in the farmer's income is $2300 per year. The farmer would then be able to afford a tractor costing up to 5000$ by paying in installments. Therefore the mechanization would be in this case financially feasible for the farmer.

The demand for a small-tractor costing up to 5000$ is estimated to be about 19,000 per year , assuming a tractor life of 8 years. The total number of tractors in Kenya is only about 11,000 at present and most of these are found on large scale farms and are not therefore available for the targeted farms. This estimate is very conservative as it does not take into account the demands of the farms with sizes between 3-5 hectares which, if growing cash-crops, would be able to afford the tractor. These farms makes about 16 percent or 240,000 farms.

CHAPTER II

ANALYSIS OF CRITICAL PARAMETERS AFFECTING A TRACTOR'S PERFORMANCE

2.1 Introduction

Tractors intended for small farm mechanization in tropical arid and semi-arid areas should be appropriately powered to match the farm sizes power requirement and should be able to develop enough drawbar pull for primary and secondary cultivation. Since the farm sizes are small, 75 % being less than 5 hectares in Kenya (see sec 1.1), the tractors intended for mechanization should be small powered and cheap enough to be afforded by the small-scale farmers.

It was therefore concluded that small-tractors with engine power output of less than 15 KW, would be a feasible mechanization tool from the point of view of farm power requirements and estimated production cost.

After having more or less picked up the tractor's engine power output, the engineering challenge would be to ensure that the operational performance of the small tractor is as good as those of medium and large tractors. On this line the first step would be to

define operational performance measures and analyse critical tractor parameters affecting its operational performance. Critical tractor parameters are parameters that either directly or indirectly affect the tractor operational performance both in terms of workrate (ha/hr) and fuel consumption (Kg/ha). These parameters also affect tractor's general performance and ownership cost.

Critical tractor parameters are going to be considered in two general grouping:

i) Parameters affecting directly tractor's operational performance.

ii) Parameters affecting general tractor performance.

2.2 Analysis of Parameters Affecting Directly Tractor's Operational Performance

2.2.1 Definitions

Drawbar pull, D (kN) : This is the pull exerted by the tractor on an agricultural implement or on a trailer.

Drawbar power. Pd (kW) : This is equal to product of horizontal component of drawbar pull D_x (kN) and tractors operational forward speed V (ms^{-1}).

$$Pd = D_x . V \ (kW) \qquad (2.1)$$

Tractive efficiency, η_d : This is the percentage of power available at the tractor axles P_A that is converted to drawbar Power Pd.

$$\eta d = \frac{Pd \times 100}{P_A} \qquad (2.2)$$

Some other quantities which are necessary for the analysis of the above parameters or would later be used during discussion have been defined for the sake of clarity , these are:

a) Specific fuel consumption gd (g/kW. h) : This is the amount of fuel consumed by the tractor per kilowatt per hour and is related to the engines specific fuel consumption in the following manner

$$gd = G/Pd = G/Pe \cdot \eta_d \cdot \eta_t = ge/\eta_d \cdot \eta_t \qquad (2.3)$$

where,

G : The amount of fuel consumed in an hour by the tractor (g).

P_d: Drawbar power (kW).

η_t: Transmission efficiency.

P_e : Engine Power Output (kW).

h_d : Tractive efficiency.

g_e : Engine's specific fuel consumption (g/kW.h).

b) Forward speed slip S : This is the ratio of speed loss to forward speed of a tractor moving without slip V_t .

$$S = \frac{V_t - V}{V_t} = 1 - \frac{V}{V_t} \qquad (2.4)$$

where

V : Actual tractor speed (ms^{-1})

V_t : Theoretical tractor speed (ms^{-1})

Tractor's operational performance measures would be defined as

(i) work-rate, π : This is the farm area cultivated by the tractor per unit time, expressed in hectares per hour.

(ii) Fuel consumption Ω : This is the fuel consumed by the tractor while cultivating, a unit farm area, expressed in kilograms per hectares.

The work-rate of a tractor pulling an implement would be given by equation (2.5)

$$\pi = 0.36\ \eta_f\ .\ W_i\ .V\ (ha/hr) \qquad (2.5)$$

where

0.36 : Conversion factor from m^2/s to ha/hr

η_f : Field efficiency, a factor to take into account the time wasted in turning the tractor around after every pass and the need sometimes to plough in an already cultivated area.

W_i : Implement width (m).

V : Tractor velocity (ms^{-1}).

Another Expression can be derived for work-rate by using the draught

of implement per unit width, K (kN/m) [5].

$$\pi = \frac{0.36\,\eta_f \cdot \eta_d \cdot \eta_t\, Pe}{K} \quad (ha/hr) \qquad (2.6)$$

The fuel consumption Ω is defined as

$$\Omega = G/\pi \,(kg/ha)$$

$$\Omega = \frac{10^4 \,.\, ge \,.\, K}{\eta_f \cdot \eta_t \cdot \eta_d} = \frac{10^4 \,.\, ge \,.\, Dx}{\eta_f \cdot \eta_t \cdot \eta_d \cdot W} \quad (kg/ha) \qquad (2.7)$$

The above equations feature tractive efficiency, drawbar pull and cultivation speed as important parameters affecting work-rate and fuel consumption. Tractive efficiency is important in that it controls the power flow between the tractor and the implement; low tractive efficiency meaning that however a good an engine (pe, ge) and transmission (η_t) the tractor has, the performance will be poor. Together with tractive efficiency, drawbar pull from a tractor are the most important parameters that will either make a particular design a success or a failure and these will be considered in more detail in the next section.

2.2.2. Analysis of Tractor Parameters Affecting Drawbar Pull And Tractive Efficiency

Many methods have been derived to analyse the relationship between various tractor and soil parameters in conjunction with drawbar pull, rolling resistance and tractive efficiency [8]. The method

adopted in this thesis is the tyre mobility number method. This method was first introduced by Freitag and was further developed by Turnage and Gee-clough et al. It has the advantage of being straightforward to use and practical [5]. Care has to be taken in using mobility number method in calculating drawbar pull produced by small tractor tyres, as tyres used in developing the empirical relationship are much larger than the small tractor tyres [6]. Here only the equations will be given, the development of the method can be found in more details in Ref. [9].

Before the method is introduced here the following definitions have to be made:

(a) Coefficient of traction, C_T :

This is defined as the ratio of tyre drawbar output D_T (kN) to the tyre load W_T (kN) as given by equation (2.8)

$$C_T T = D_T / W_T \qquad (2.8)$$

(b) coefficient of rolling resistance C_R :

The coefficient of rolling resistance is defined as the ratio of the rolling resistance, R_T (kN) experienced by a rolling tyre to the tyre load W_T as given by equation (2.9)

$$C_R = R_T / W_T \qquad (2.9)$$

(c) Maximum coefficient of traction C_m :

The coefficient of traction increases with increase in tyre slip reaching a maximum at s=100%. The maximum coefficient, C_m, is therefore defined as the coefficient of traction at s=100%;

$$C_m = D_T / W_T \text{ (at } s = 100\ \%\text{)} \qquad (2.10)$$

The tyre mobility number method is based on defining a non-dimensional number, M_T , as given by equation (2.11) and empirically by deriving a relationship between the tyre mobility number and coefficient of traction with slip.

$$M_T = \frac{C\,b\,d}{W_T} \sqrt{\frac{\delta}{h}} \left(\frac{1}{1 + \frac{b}{2\,d}} \right) \qquad (2.11)$$

Where,

C : Soil cone index value (kN / m^2).

b : Tyre width (m)

d : Tyre diameter (m).

W_T: Tyre load (kN)

δ : Tyre deflection (m).

h : Tyre section height (m).

The variation of coefficient of traction C_T with tyre slip, s, is given by equation (2.12)

$$C_T = C_m \ (1 - e^{-Ks}) \qquad (2.12)$$

where the wheel slip, s is in decimal and K is a rate constant whose relationship with the tyre mobility number will be given later. The maximum coefficient of traction, C_m is related to mobility number by Equation (2.13)

$$C_m = 0.796 - \frac{0.92}{M_T} \qquad (2.13)$$

The relationship between the tyre mobility number M_T and the rate constant was empirically found as given by equation (2.14)

$$K \cdot C_m = 4.838 + 0.061\ M_T \qquad (2.14)$$

The coefficient of rolling resistance C_R is related to the mobility number as shown by the equation (2.15)

$$C_R = 0.054 + 0.323\ /M_T \qquad (2.15)$$

Equation (2.15) is valid for tyres of diameter ranging between 0.8-0.95 m, for tyres of other sizes, Gee-clough et al [9] should be consulted.

Once the coefficients of traction and rolling resistance are determined, then a driving tyre's drawbar pull and a towed tyre's rolling resistance are given by equations (2.16) and (2.17) respectively.

$$D_T = C_T \cdot W_T \qquad (2.16)$$

$$R_T = C_R \cdot W_T \qquad (2.17)$$

Thus the tractor's drawbar pull D can be determined by summing the drawbar pull outputs of each driving tyre and subtracting the force required to overcome the rolling resistance, as given by equation (2.18)

$$D = \sum_{i=1}^{n_d} C_{Ti} W_{Ti} - \sum_{i=1}^{n_t} C_{Ri} W_{Ti} \qquad (2.18)$$

where

n_d : Total number of tractor's drive tyres

n_t : Total number of tractors tyres

C_{Ti} : Coefficient of traction for each drive tyre

W_{Ti} : Load acting on each tyre

C_{Ri} : Coefficient of rolling resistance for each tyre

The tractive efficiency n_d is then given by equation (2.19)

$$\eta_d = \frac{D(1 - s)}{D + \sum C_{Ri} \cdot W_{Ti}} \times 100 \qquad (2.19)$$

The equations above show that high tyre drawbar pull output D_T and low rolling resistance R_T are obtained for large values of mobility number M_T. Equation (2.11) shows that the mobility number is directly proportional to tyre width and diameter, thus tyre drawbar pull D_T and tractive efficiency could be a increased by using tyres with larger diameter and width. The equations (2.8 - 2.19) will

be used to assess the performance of a small 4-wheel tractor in arid and semi-arid agriculture so as to analyse its suitability in the mentioned agricultural areas.

2.2.3 Tractor's Cultivation Speed

Tractor's cultivation speed is an important parameter that affects the tractors operational performance in terms of its work-rate as is given by equation (2.5)

$$\pi = 0.36\, n_f\, W_i\, .\, V \quad \text{(ha/hr)} \qquad (2.5)$$

It is therefore of paramount importance to optimize the cultivation speed while considering the following constraints.

(i) Low cultivation speed results in low percentage engine power utilization as would be explained in details later. This is because the drawbar pull output of drive tyres are independent of speed (see sec 2.2.2) and that operations at higher speed result in higher drawbar power output as shown in equation (2.1).

(ii) High cultivation speed results in increased implement draught requirements as the draught forces vary directly with speed for same implement [6], while squarely for others [7]. Increased draught forces mean increased energy use per unit area of cultivation and thus a higher fuel consumption, Ω.

2.3. Analysis of Parameters Affecting the General Tractor Performance

Though there are many parameters affecting the general tractor performance the most important two would be considered here and these are

i) Stability and Steerability

ii) Ergonomic considerations

2.3.1. Stability and Steerability

The tractor design would naturally affect the modes of tractor instability and steerability, and henceforth the analysis of the mode of tractor instability and condition of insteerability would be required while taking each particular designs into consideration. The different design to be considered include;

i) Single-axle tractor with implement

ii) Conventional 4-wheel tractor

2.3.1.1. Single-Axle Tractor With Implement

a) Stability

For a single-axle tractor working on a slope. The static lateral instability would arise when

$$\text{Tan}\beta = T_A / 2\,G_A \qquad (2.20)$$

where β : The limiting slope angle

T_A : Tractor wheel track

G_A : Height of center of gravity

Single-axle tractors are unlikely to experience any other mode of instability except the one discussed above.

b) Steerability

Though conditions of insteerability for single-axle tractor with an implement attached does not result in fatal accidents as is the case for four-wheel tractor's, nevertheless , it affects tractor's work rate adversely.

Single axle tractors can, for the sake of simplicity be divided into either large or small category .The small single axle tractor would have 3-5KW petrol engine and a solid axle. The larger single axle tractors have 7-10 KW diesel engines, multiratio gearboxes and steering clutches. Steering of these tractors is difficult and tiring [4] ,as this machines tend to sway during cultivation due to either the drawbar pull not acting centrally or the variation of rolling resistance experienced by the wheels; and to steer the operator is required to apply a force [11].

2.3.1.2. Conventional 4-Wheel Tractor

a) Stability

Conventional 4 wheeled tractor can experience any of the modes

of instability mentioned below

i) longitudinal instability (rearing tendency)

ii) lateral instability

i) Longitudinal Instability (rearing tendency)

Longitudinal instability results when a tractor's front tyres rise and lose contact with the ground [12]. The position of drawbar pull application is among the most important variables affecting tractors static longitudinal stability. The longitudinal stability of a tractor can be increased by the adding weights to the tractor chassis in order to move the center of gravity forward and lower it.

ii) Lateral Instability

This is a term applied for sideways overturning of tractor. Here only static lateral instability would be considered. For a tractor working on a slope, the limiting slope angle β_r for one of rear wheel to loss contact with the ground and initiate an overturn is given by the eguation (2.20) below. [13]

$$\text{Tan}\,\beta_r = \frac{T_2\,(W - B)}{2\,H_1\,(W - B\,H_2 / H_3)} \qquad (2.21)$$

The limiting slope angle b_f for one of the front wheels to loose contact with the ground is given by equation (2.21)

$$\text{Tan}\,\beta_f = T_1 / 2\,H_2 \qquad (2.22)$$

where:

T_1 = Front track, (m).

T_2 = Rear track, (m).

H_1 = Horizontal distance of center of mass from rear axle, (m).

H_2 = Pivot point height, (m).

H_3 = Height of the center of mass of vehicle plus pay load (m).

W = Vehicle wheelbase (m).

B = Horizantal distance of center of mass from rear axle, (m).

b) Steerability

Conditions of insteerability can be defined as conditions when tractor's driver loses tractor's directional control. Such conditions can result when

i) The front tyres are no longer capable of producing the lateral force necessary for directional control.

ii) Rear wheels slip sideways

iii) Trailer slides sideways if trailer is attached

The most important factor that causes poor steerability and which may have fatal consequences is the inability of the tractors front wheel to develop the required steering force for directional control. Gee-clough et al (1981) [14] showed that soil and tractor parameters affecting steering force from an angled undriven wheel are much the same as these affecting drawbar pull and tractive efficiency discussed in section 2.2.2.

Tyre mobility number method is also used to model the relationship between various tractor and soil parameters affecting the steering force from an undriven angled wheel.

Though there are various mobility numbers defined, only the one defined by equation (2.23) gives the best correlation between the experimentally found steering forces and those derived by using the modelling equations. The definations of the other three modelling equation could be found in more detail in Ref [14].

The tyre mobility number M_s to be used for predicting the steering force is a modification of equation (2.11) as

$$M_s = \frac{C\,b\,d}{W_T}\sqrt{\delta/h}\left(\frac{1}{1+b/2d}\right)\theta^n \qquad (2.23)$$

where:

c = Soil cohesion (kPa).

b = Tyre width (m).

d = Tyre diameter (m).

W_T = Tyre load (kN)

δ = Tyre deflection (m).

h = Tyre section height (m).

ϕ = Soil internal friction

n = Exponential constant (n = 1.35).

Before introducing the equation to be used for predicting the steering force the following definitions have to be made.

(a) Coefficient of steering force C_S .

This is the ratio the steering force S_T produced by an angle tyre to the tyre load W_T as defined by the equation (2.24) below.

$$C_S = S_T / W_T \qquad (2.24)$$

(b) Maximum coefficient of steering force C_S.

This is the ratio of steering force S_T at tyre slip angle α equal to 1.22 radians to its tyre load W_T, defined by equation (2.25).

$$C_{sm} \frac{S_T}{W_T} \qquad (\alpha = 1.22 \text{ radian}) \qquad (2.25)$$

The empirically derived relationship between the coefficient of steering forces C_S, the maximum of steering force and the tyre slip angle α is given by equation (2.26)

$$C_S = C_{Sm} [1 - \exp(- K\alpha)] \qquad (2.26)$$

The relationship between maximum coefficient of steering force C_{Sm} and M_S is given by equation (2.27)

$$C_{Sm} = 0.86 - 0.6 M_s \qquad (2.27)$$

The rate constant K was found empiricially [14] to be related to the tyre mobility number as given by equation (2.28) below

$$K.\ C_{Sm} = 2.39 + 53.50\ M_s \qquad (2.28)$$

The coefficient of rolling resistance for an undriven angled wheel varies with the tyre slip angle α and could be modelled as given by the eguation (2.29) below

$$C_R = C_{Rm}\ (1 - m\ a) \qquad (2.29)$$

where C_{Rm} is the maximum coefficient of rolling resistance for zero tyre slip angle and m is a constant which varies between 0.05-0.12. The relationship between maximum coefficient of rolling resistance and tyre mobility number is given by eguation (2.30).

$$C_{Rm} = 0.0014 + \frac{0.0057}{M_S} \qquad (2.30)$$

The steering force acting on an undriven angled tyre is then given by using equation (2.24) and rewriting it as

$$S_T = C_S\ .\ W_T \qquad (2.31)$$

While the rolling resistance can be obtained by using equation (2.9), equation (2.29) and equation (2.30). After having found both the steering force and the rolling resistance, the steerability of the tractor could be checked. The equations (2.23-2.31) will be used to assess the steerability of a small-4 wheel tractor in different soil conditions, in chapter IV.

CHAPTER III

SUITABILITY OF SINGLE-AXLE TRACTORS AND WINCH-POWERED CULTIVATION DEVICES FOR SEMI-ARID LAND CULTIVATION

3.1 Introduction

It was concluded in the previous chapter that a small tractor with an engine power output of 10-15 KW will be a feasible mechanization tool for small-farm holders based on economic and social conditions in Kenya. This fact has long been recognized by many research institutes and manufacturing companies that are concerned with developing a mechanization tool for small farm holders in different parts of the world. As expected, these attempts came up with different types of small tractors each suited to a particular agricultural practice, climatic condition or crop. These different small tractor types include single-axle tractor, winch type tractor and 4-wheel, ride-on small tractor.

Of the above mentioned small tractor types, only the winch-type tractor was developed for arid and semi-arid mechanization but was never commercially produced. It could be therefore be stated safely that these particular agricultural regions

await a new and innovative solution for their desperately needed mechanization program.

In order to give a better view of the work aimed at in this thesis, an evaluation will be made between the above mentioned small tractor types as alternatives for arid and semi-arid region agricultural mechanization. The evaluation is based on the methods and performance criteria introduced in the previous chapter.

For the sake of brevity, winch-type and single-axle tractors are going to be considered in this chapter. It was found more appropriate to discuss 4-wheel ride-on tractors under a separate heading.

In this chapter, the assessment of the suitability of these tractors for arid and semi-arid regions will be done under the following headings

(i) Single-axle power tillers

(ii) Tractive type single-axle tractor

(iii) Winch-type tractor.

3.2 Single-axle Power Tillers.

The single-axle power tillers were first introduced in Japan around 1950. These tractors achieved widespread popularity and were in use early 1970's in 3 out of 5 million farms in Japan [16] . They have also been widely used in other East Asian countries

practicing wetland rice culture on small farms. These tractors have the advantage of achieving both Ploughing and harrowing in the same pass of the machine on the field and function by cutting and stirring up the soil [17].

The figure below shows sketch as of a single axle power tillers

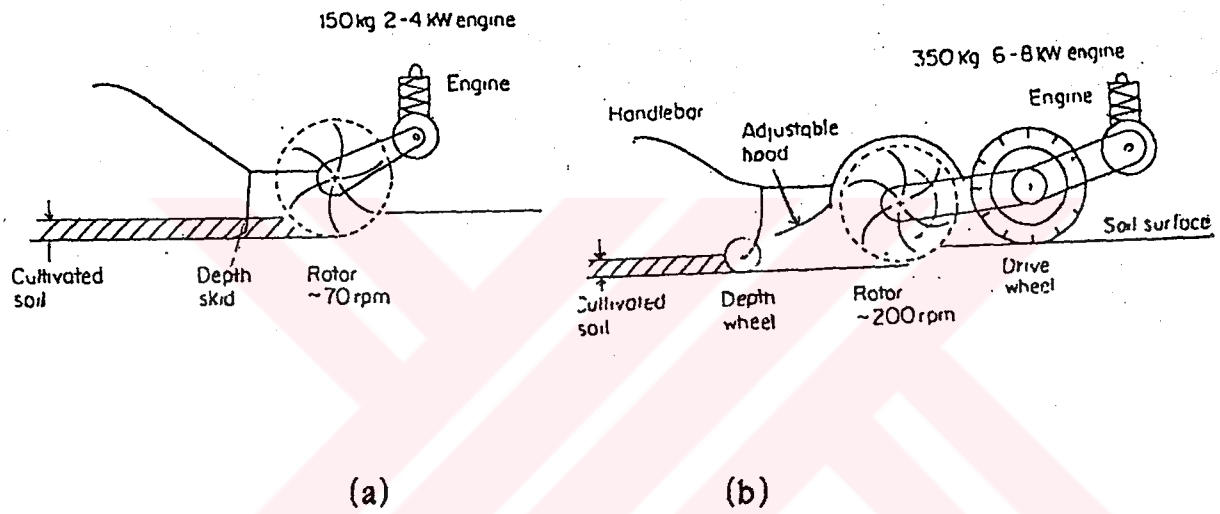

Figure 3.1 Schematic Diagrams of Single Axle Power Tillers [4]

Despite their success in countries practicing wetland rice culture in small farms, these tractors cannot be used to perform primary cultivation in arid land cultivation due to excessive hardening of the soil after dry season; for they experience excessive vibrations and blade wear[3]. Apart from seedbed preparation and in the limited areas practicing wetland rice culture, these tractors cannot contribute to mechanize agriculture in Kenya.

3.3 Tractive Type Single-Axle Tractors.

Tractive type single axle tractors have also achieved wide acceptance in East Asian countries. Many countries have designed and manufactured their own tractive type single-axle tractors, the most recent examples being Kenya [18] and Mexico [11] which have both unveiled locally designed and manufactured tractors. It is hoped that these tractors would help in small scale farm mechanization effort. A sketch of this type of tractor is given in figure 3.2 below.

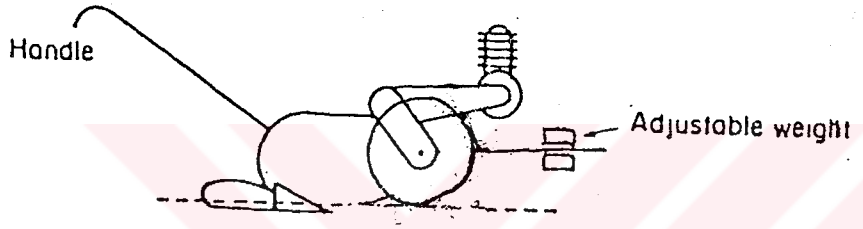

Figure 3.2. A Sketch of Tractive Type Single Axle Tractor.

The prices of single-axle tractors range between 1038 $ to 2178 $ depending on the country of manufacture [11, 19]. These prices are vary low when compared to those of medium powered tractors (40-60 HP) and thus, from cost point of view are feasible means of mechanization for land cultivation.

The suitability of these tractors for arid and semi-arid region cultivation could be analysed by considering

(i) Operational performance

(ii) General tractor performance

(i) Operational performance

Single-axle tractors would have very poor operational performance when used in arid and semi-arid regions as their work-rate and quality of work would be very low. This is mainly because these tractors have very low drawbar pull due to their small tyres and light weight. In a study carried out by Erdoğan [20] the drawbar pull of a single axle tractor weighing about 2500 N was found to be about 1000N at 15% tyre slip. This result is not much different from the result obtained by Lara-Lopez et al [11], where the drawbar pull of a single axle tractor weighing 4700N and operating at a soil having cone index value 818kPa was found to range between 1700-2100N at 12.3 % tyre slip.

The predicted drawbar pull using mobility number method introduced in the previous chapter for single-axle tractors weighing up to 5000N, having tyre sizes 6.00-16 and operating in a soil with cone index value 814 kPa at 12.3 % tyre slip is about 1960 N; which is in conformance with those found by Erdoğan [20] and Lara-Lopez et al [11]. It is worthwhile pointing out that the tractor mentioned in ref [18] is just a prototype, no information pertinent to it's field performance was given.

It is therefore clear that tractive type single-axle tractors cannot be used to mechanize arid and semi-arid region as it drawbar pull is insufficient and falls far short of the minimum required 5000N draught force [4] for primary cultivation.

(ii) General tractor performance

In areas with soft soils, single axle tractors can produce the required drawbar pull for primary cultivation but due to it's inherently poor ergonomic design, when compared with a 4-wheel ride on tractor with the same engine output, these tractors have a much lower general performance in terms of higher utilization hours per day (about 3 hours/day [4]).

It is clear from the foregoing discussion that, wherever possible, 4-wheel ride-on tractors should be introduced as mechanization tool for small-farm holders, as it has a higher general performance than a single-axle tractor for the same engine power output.

3.4 Winch-Type Tractor

In order to overcome the low drawbar pull of tractive type single-axle tractors, winch-powered cultivation devices have been an attractive solution [21]. The device basically consists of a small self-propelled winch and a separate implement. It requires 2 people to operate . The diagram below shows outline of a self propelling winch and a winch-pulled implement.

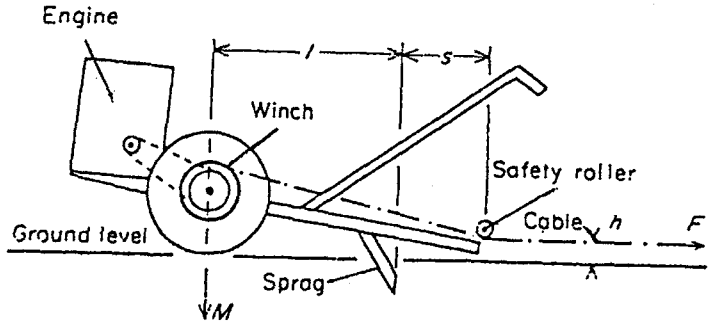

Figure 3.3 An Outline of a Self-Propelled Winch

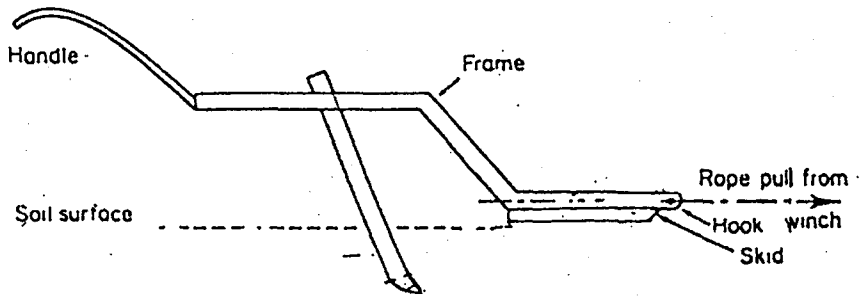

Figure 3.4. A Winch-Pulled Implement

Operation principle of the winch-type tractor is that the self propelling winch is driven across the field until the end of the field or cable (whichever comes first), the machine is then stopped and the winch is engaged pulling the implement across the field. The process is then repeated. The machine has a very low work-rate. The price of the machine is not much different from that of a single-axle tractor, it is about 1700$.

The suitability of winch-type tractor for arid semi-arid region could be assessed by considering it's operational performance.

Operational Performance

This tractor's operational performance is low as it has a low work-rate. The tractor's work-rate is about 0.2 ha/day, which is equivalent to that of a pair of oxen. The main causes of such a low work-rate are that the cultivation speed is low. (about 0.7 ms^{-1}) and the greater percentage of time being spent in positioning of the

self-propelling winch prior to engaging it into the winching mode and pulling the implement across the field. In a typical farming conditions it is expected work-rate would be much lower. Because the above mentioned work-rates are extrapolated from experimental work-rate values obtained from on small fields, they do not include the effect of operator fatigue.

Despite the fact that winch-type tractor has the capability to produce a drawbar pull of 5000N, it was found that the operational performance was too low and that a 4-wheel ride-on small tractor of the same engine power output would have much higher operational performance particularly in terms of work-rate.

In Summary

a) Winch-type tractor do not rely on weight to provide the required drawbar pull but are not promising solutions in view of their low work-rate. Furthermore their poor operational performance is not offset by low price.

b) Single-axle tractors are dismissed as the solution of the problem on account of low traction, though it can be argued that their tractive effort could be improved by improving the coefficient of traction. But this is not an overall feasible alternative in view of their poor general performance, namely poor steerability.

In conclusion it is most feasible to investigate the second alternative (improving tractive coefficient) to ride-on small tractors which is the subject matter of the following chapter.

CHAPTER IV

ASSESSMENT OF THE PERFORMANCE OF BAŞAK TRACTOR IN ARID AND SEMI-ARID REGION

4.1. Introduction

In the foregoing chapter, the performance of single axle tractors and winch-type tractor were investigated and both were found to be unsuitable as mechanization tools for arid and semi-arid region cultivation. In this chapter the performance of a 4-wheel ride-on tractor will be assessed.

The tractor chosen for the assessment is Başak-17. This is a locally produced tractor by Türkiye Zirai Donatım Kurumu. It is a two wheel drive, 17-horsepower tractor. Başak-17 tractor is shown in Figure 4.1 [22]. The tractor's technical specifications which would be used during the assessment process are given in Table 4.1 [22, 23].

The operational performance of the Başak tractor is measured by using the criteria developed in chapter II; ie work-rate in hectare

Figure 4.1. Başak-17 tractor

per hour and fuel consumption in kilogram per hectare. Due to lack of detailed engine performance data, the fuel consumption of Başak-17 could be calculated and thus operational performance would be measured by using the work-rate only, of course it is futile to discuss operational performance without ascertening whether the tractor can perform primary and secondary cultivation. Therefore the first step would be to check whether the tractor can develop the required drawbar pull for primary and secondary cultivation and this would be done in section 4.2.

Table 4.1 Başak Tractor's Technical Specifications

Model	:	Başak -17
Engine	:	
Mark and Model	:	Lombardini, 4LD 820 automotive type
Max power output	:	17 horsepower
Engine rpm	:	3000 rpm (max power)
Max torque	:	5 Kg.m (at 2200 rpm)

Gearbox, and Differential						
Gearbox type	:					
Number of gears	:	4 forward and reverse				
First gear speed	:	3.17 Km/h				
Maximum speed	:	15.66 Km/h				
Gear ratios	:	1	2	3	4	reverse
Speed (MKm/h)	:	3.17	6.27	10.35	15.66	4.98

Brake type	:	Mechanical

Fuel type	:	Diesel
Fuel tank capacity	:	10 litres

Tyres			
Rear tyres	:	7.00 x 18	tractive type
Front tyre	:	4.00 x 12	implement type

Tractor weight on front axle	:	229 Kg
Tractor weight on rear axle	:	470 Kg.
Total tractor weight	:	699
Additional weights on front axle	:	21 Kg.
Additional weights on rear axle	:	80 Kg.
Total tractor weight with additional weight	:	800 Kg.

Power take off	:	
P.T.O (rpm)	:	540 rpm.

4.2 Başak Tractor's Drawbar Pull and Tractive Efficiency

Tyre mobility number method introduced in section 2.2.2 was employed to determine Başak tractor's drawbar pull and tractive efficiency. Due to the fact that the tractor would be used in various seasons and thus at various soil moisture content and soil condition, the drawbar pull should vary accordingly. Thus, Başak tractor's theoretical performance was determined for five different soil

conditions typically met in farm land. These are given in Table 4.2 together with their cone index value.

Table 4.2 Cone Index Values of Typical Farmland Soils [10].

Soil Condition	corresponding cone index value (kPa)
wat, loose	200
Dry loose	400
Wet, stubble	500
Dry, stubble	1000
Dry, grasland	1500

Equations (2.8-2.19) were used to draw graphs for drawbar pull and tractive efficiency vs wheel slip for the five different soil conditions represented in Table 4.2. These graphs are given in Figures 4.2 and 4.3.

It is important to point out that a tractor's wheel slip is a function of implement draught requirement and drive wheels' drawbar pull output. As it can be followed from equation (2.12), the higher the wheel slip (s), the greater the coefficient of traction and thus drive wheel's drawbar pull. In other words, as the implement draught requirement increases, so does the tractor's drive wheel slip until the wheels' drawbar pull balances the implement draught, and tractor's wheels rolling resistance or the tractor is stationary and the wheels rotating without tractor's forward displacement.

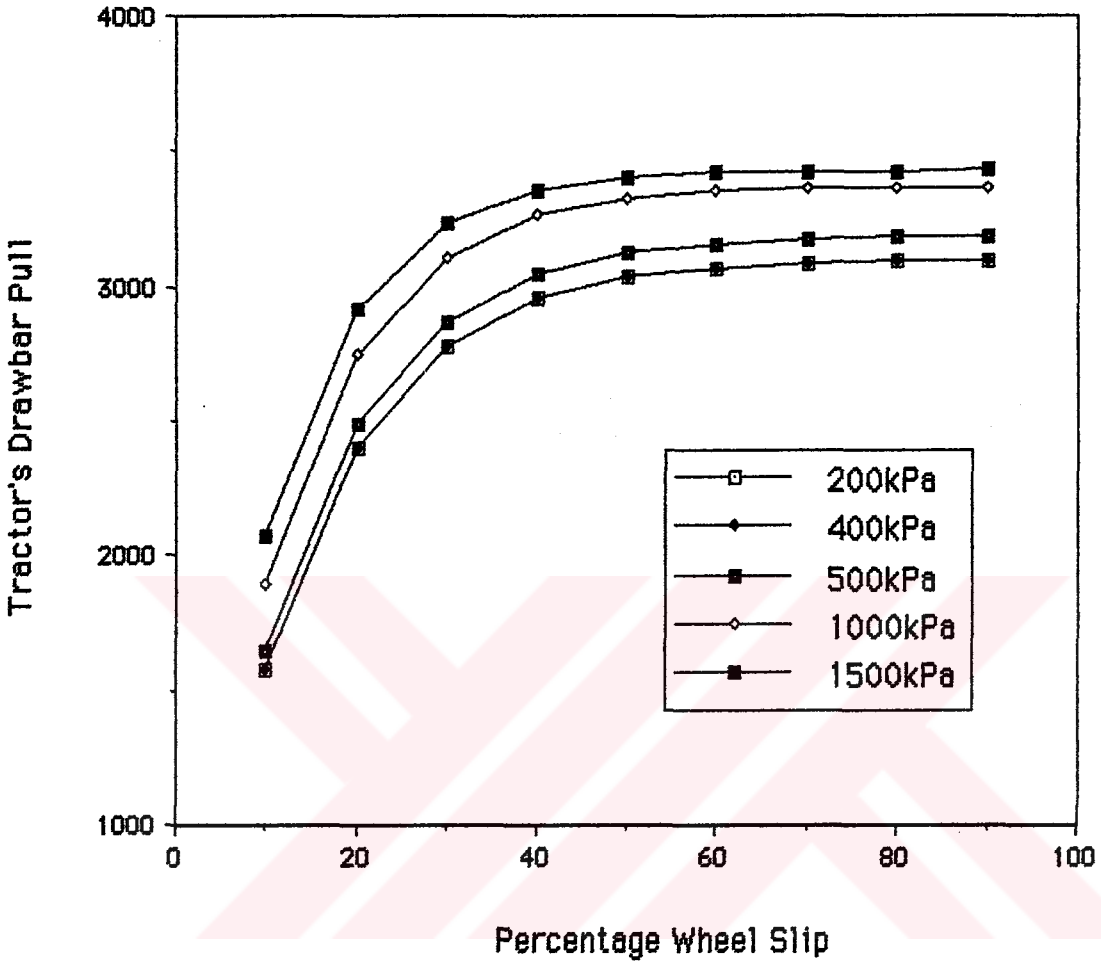

Figure 4.2.The Drawbar Pull of Basak-17,Operating in Soil Whose Cone Index Values are Shown in the figure

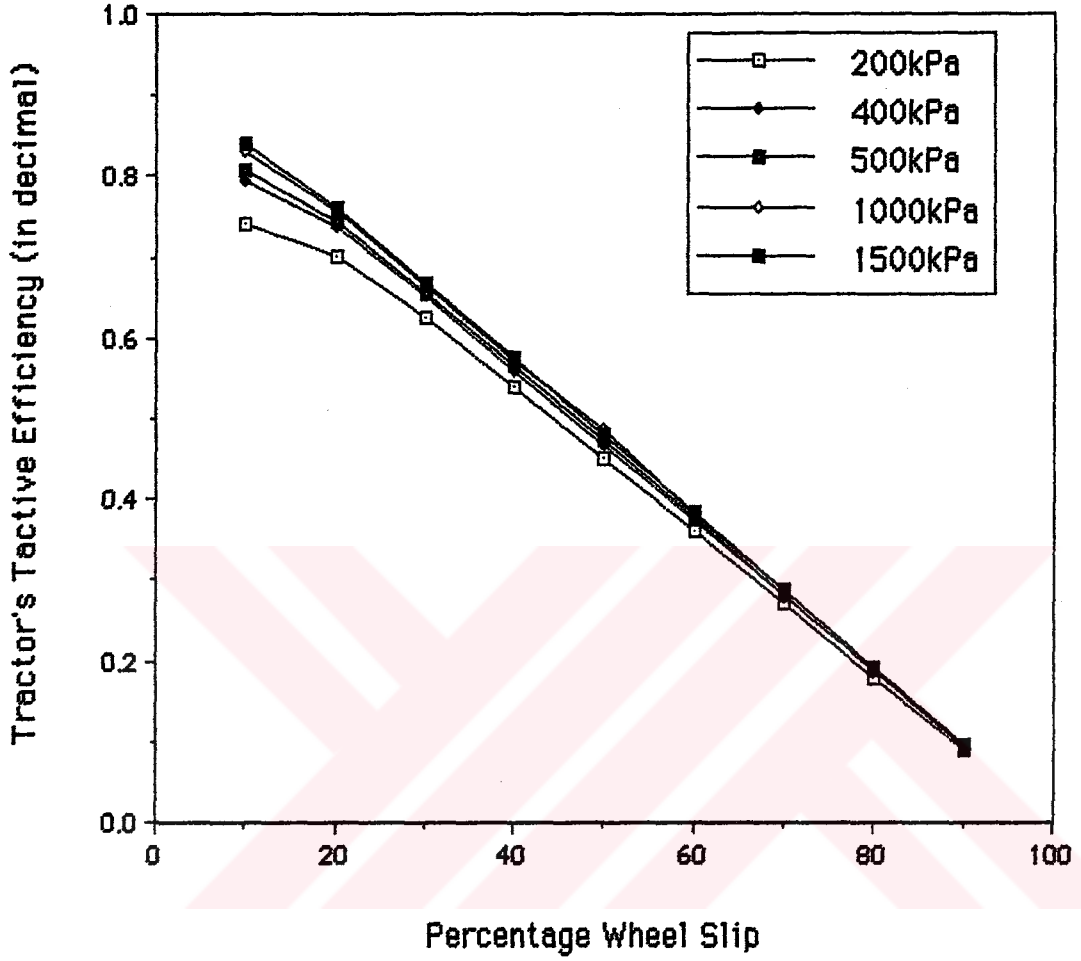

Figure 4.3.The Tractive efficiency of Basak-17,Operating in Soil Whose Cone Index Values are Shown in The Figure.

For practical purpose's the tractors are assumed to have wheel slip between 15-25 % [20]. Which will be referred to as operational wheel slip throughout the thesis. This range of wheel slip was adopted for the assesment of Başak tractor's drawbar pull and tractive efficiency.

Figure 4.2 shows that at the operational wheel slip, the highest drawbar pull that can be developed by Başak-17 is under 3 kN for all soil conditions except for soils with cone index value greater 1500 kPa. Clearly Başak-17 tractor cannot then be used for primary cultivation in arid and semi-arid land where the implement drawbar pull requirement is in excess of 3-5 kN [10]. Due to lack of any feasible alternative to 4-wheel ride-on small tractors for mechanization of arid and semi arid region, the necessary modification to these tractors in order to develop the required drawbar pull will be discussed later in this thesis.

Nevertheless drawbar output of this tractor is enough to operate secondary cultivation implements, thus the performance of this tractor would be assessed while performing secondary cultivation in the following section.

4.3. Assessment of Tractor Performance for Secondary Cultivation

4.3.1 Workrate

Secondary cultivation is termed as turning an already disturbed soil into a seedbed suitable for planting [4]. Therefore the tractor's performance would be assesed on loose soil which has cone index values between 200 kPa and 500 kPa.

Crossley et al [10] found that for arid regions the maximum drawbar pull required to perform secondary cultivation is about 2kN.

The tractor is work-rate is calculated for three wheel slip values and these are 10%, 20% and 30% and tractor speed at first and second gear. The work-rate is calculated by using equation (2.5) below.

$$\pi = 0.36\ \eta_f\ .\ W_i\ .\ V \text{ (ha/hr)}$$

or (2.5)

$$\pi = 0.36\ \eta_f\ .\ W.V_t\ (1-s) \quad \text{(ha/hr)}$$

The work-rate per day is found by using an eight hour working day.

The working day values of tractor's working rate is tabulated for different wheel slip and tractor speed in Table 4.3.

Table 4.3. Tractor's Work-rate

wheel slip value %	Soil condition and cone index value	work-rate at first gear (ha/day)	work-rate at second gear (ha/day)
10	disturbed soil	0.54	1.08
20	200-500 kPa	0.49	0.96
30		0.43	0.84

The work-rate values were calculated by assuming that a mouldboard plough of width 300 mm was used. Values found in the literature for arid land cultivation using moulboard plough in semi-arid regions are not much different. Crossley et al [10] found experimental values of about 0.78 ha/day and 0.68 ha/day.

4.3.2 Percentage Engine Power Utilization

Figures 4.4-4.5 were plotted to illustrate the percentage of engine power utilized by the Başak tractor while performing secondary cultivation. The performance displayed by the graphs are very interesting in the sense that for Başak Tractor, at best conditions, the drawbar power is only 30% of the engine power available for utilization. When operating at wet and loose soil of cone index value about 200 kPa, the maximum drawbar power is only 13% of engine power available for utilization.

The conclusion that can be reached from studying the graphs in figures 4.4-4.5 is that the tractor's actual per formance does not justify a 17 HP engine and that the tractor would have displayed the same performance had it had a 9-horsepower engine; provided that the axle loads were kept constant. From a different angle, is the farmer pays for an engine he only uses half of is capacity and this is a source of loss to a farmer. This may be one of the reasons why Başak lost its popularity.

The utilization of less than half of the engine power available for farming is an unacceptable condition even if the drawbar pull of the tractor is enough to operate both primary and secondary cultivation implements. Therefore, on this point alone, Başak-17 needs to be modified so as to enable the user to achieve much higher engine power utilization, such a modification would be discussed later in this thesis.

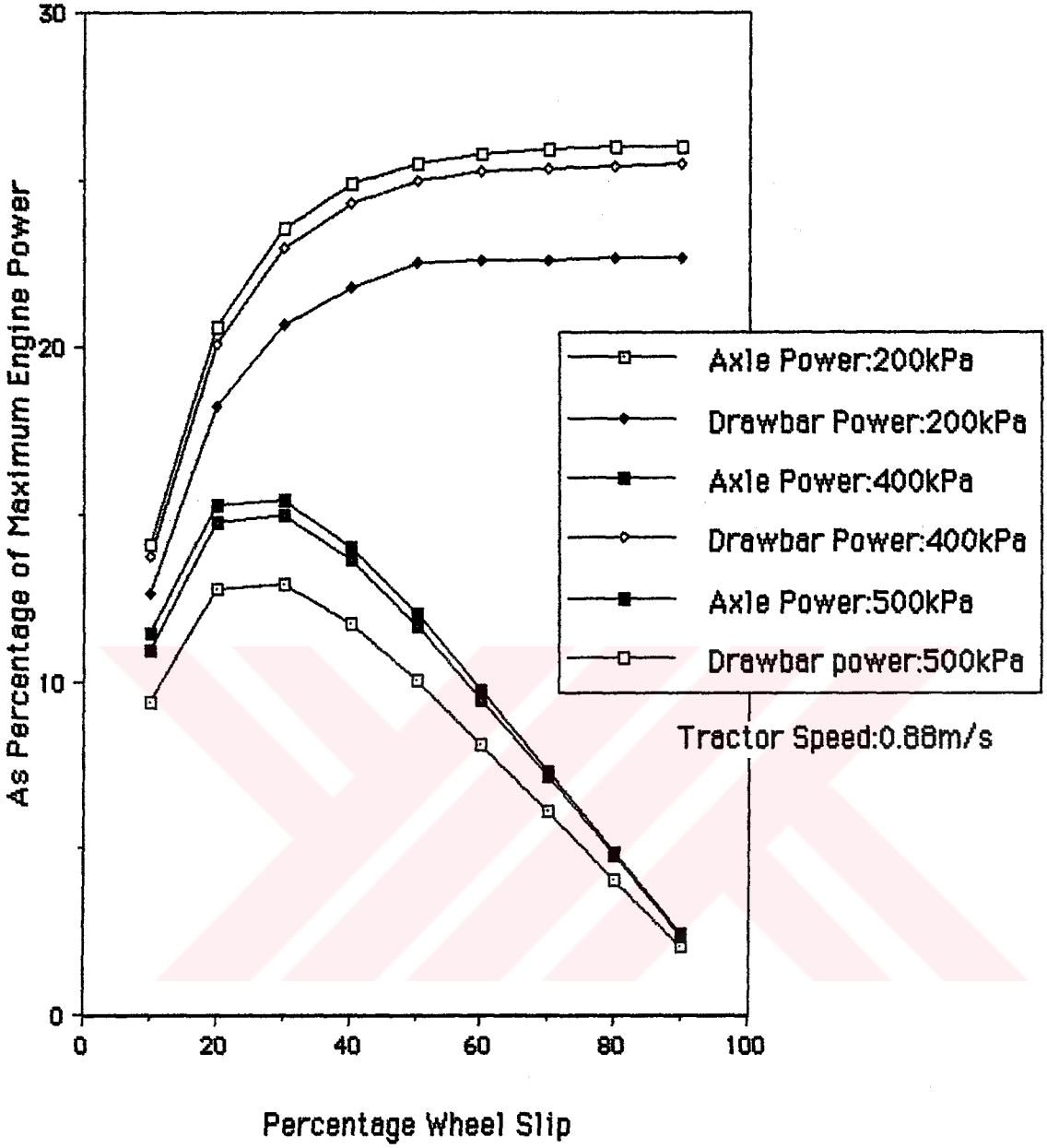

Figure 4.4.Drawbar Pull and Axle power as Percentage of Maximum Engine Power for Basak-17,Operating in Soils Whose Cone Index Values are Shown in The Figure.

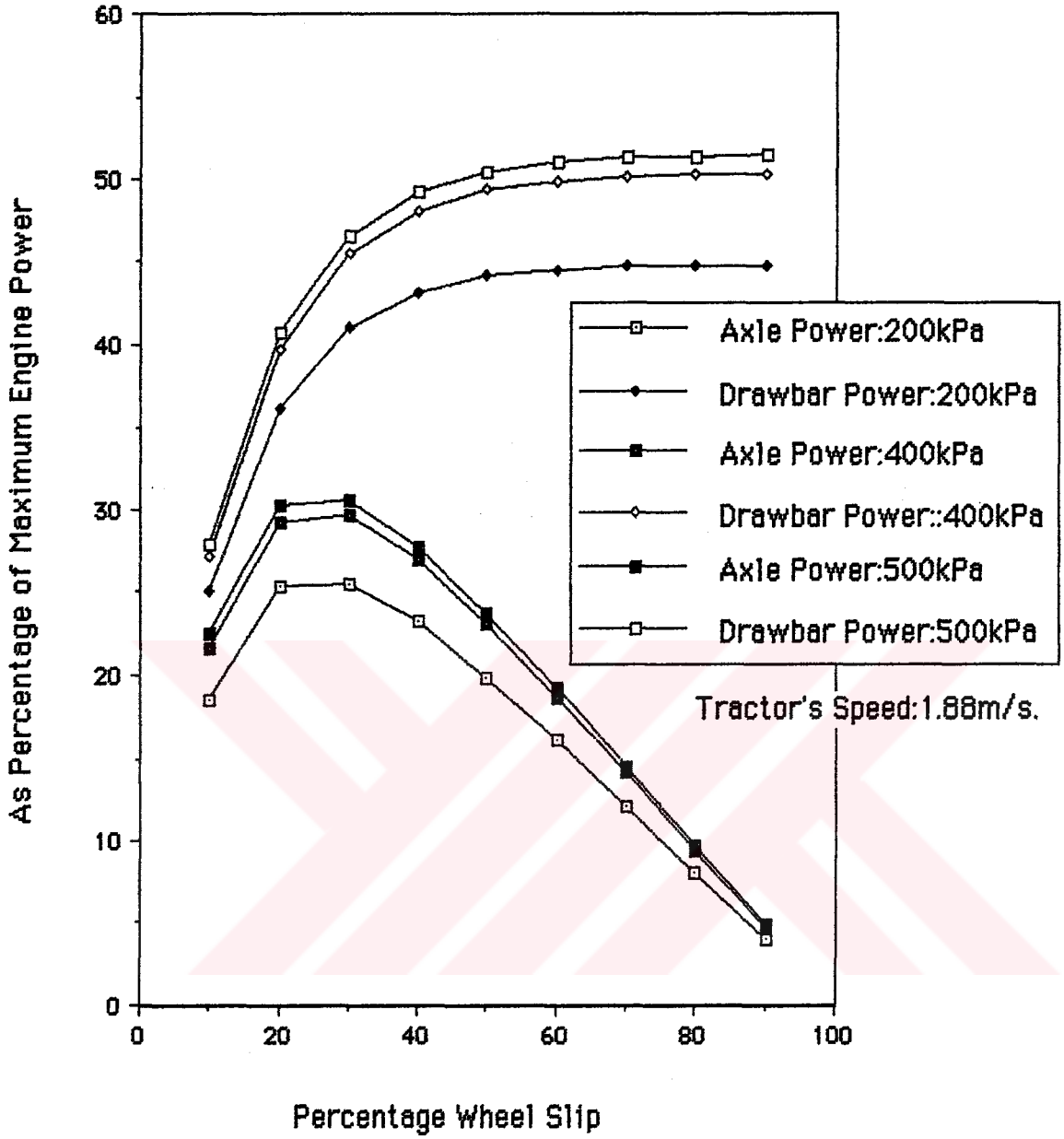

Figure4.5.Drawbar Power and Axle Power as Percentage Engine Power for Soils Whose Cone Index Values are Shown in The Figure

4.3.3 Tractor Stability

As mentioned earlier a ride-on tractor's stability is one of the important parameters affecting the tractors general performance. Tractor's stability can be divided into two, longitudinal stability and lateral stability. Here only lateral stability would be investigated as it occurs most commonly.

Tractors are required to operate on slope with a slope angle up to 15° [10]. Equation (2.21) would be used to find the limiting slope angle β_r for rear end overturning for Başak-17, equation (2.21) is written below as

$$\tan \beta_r = \frac{T_2 (W - B)}{2 H_1 (W - B H_2 / H_3)} \qquad (2.21)$$

while the limiting slope angle bf for front end oveturning is given by equation (2.22) below

$$\tan B_f = T/2 H_2 \qquad (2.22)$$

The parameters given in equations. (2.21-22) for Başak-17 are given in Table 4.4

Table 4.4. Tractor's Dimensions Required for Stability Analysis [23].

	Symbol	(mm)
Front track	T_1	840
Rear track	T_2	1006
Tractor wheelbase	W	1385
Horizontal distance of center of mass from rear axle	B	453.7
Pivot point height	H_a	380
Horizontal distance of pirot point from rear axle	H_3	1385
Height of center of mass of vehicle plus payload	H_1	450

By substituting the values of the parameters into equations (2.21-22), the limiting slope for Başak-17 is found as β_f =18.65o and β_f =47.86. Therefore the stability of Başak-17 is acceptable.

4.3.4 Tractor's Steerability

The steerability of this tractor would be checked for soil conditions given in Table 4.5 [14]. Which are not much different from those at which percentage power utilization graphs in figures 4.4-4.5 were drawn.

In steerability analysis, the implement weight transfer is ignored and it is assumed that the implement is a drawn type and not a hitched type.

Table 4.5 Cone Index Values of Soils Found in Cultivated Farmland

Nominal cone index	Cone index value measured	Soil Cohesion C (kPa)	Interval friction angle Q°	Addesion of soil to rubber Ca (kPa)	Soil-rubber friction angle δ^{0}	Specific weight μ (CN/m)
150	128	2.17	25.7	1.22	22.8	13.05
300	284	4.35	32.7	0.52	24.8	14.22
550	577	6.89	37.1	0.36	26.9	15.30

Figure 4.6 shows the forces acting on Başak-17 when turning. The center of gravity of the tractor is at 0. The total turning moment about the center of gravity would be.

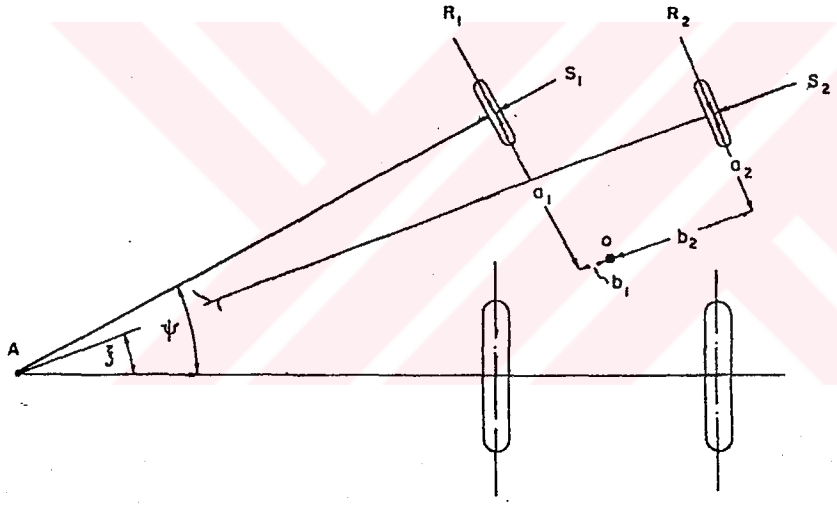

Figure 4.6 Forces on Başak-17 Tractor's Front Wheel When Turning.

$$MO = S_1 a_1 + S_2 a_2 + R_1 b_1 - R_2 b_2 \qquad (4.1)$$

For the sake of simplicity let y = t then S1 = S2 and R1 = R2 therefore equation (4.1) becomes

$$MO = S (a_1 + a_2) + R (b_1 - b_2) \qquad (4.2)$$

The values of (a_1 + a_2) and (b_1 - b_2) for various major steering angles ψ are shown in Table 4.6.

Table 4.6 Side Force Moment Arm and Rolling Resistance Moment Arm for Major Steering Angles 10°, 20° and 30°.

Major steering angle Ψ	Side force moment arm ($a_1 + a_2$) mm	Rolling resistance Moment arm ($b_1 - b_2$) mm	Ratio $\frac{(a_1 + a_2)}{[(b_1 - b_2)]}$
10	72	- 13	5.538
20	68	- 26	2.615
30	64	- 37	1.729

By the use of equation (2.23-2.31), the variation of the ratio of the side force S and the rolling resistance R were drawn for tyre slip angle upto 70° as shown in Figure 4.7. It is apparent from Figure 4.7 and Table 4.6 that for all soil conditions and tyre slip angle above 10 % the product of side force moment arm and side force is an order of magnitude greater than the product of rolling resistance moment arm and rolling resistance. Therefore the tractor would be steerable in all the soil conditions shown in Table 4.5.

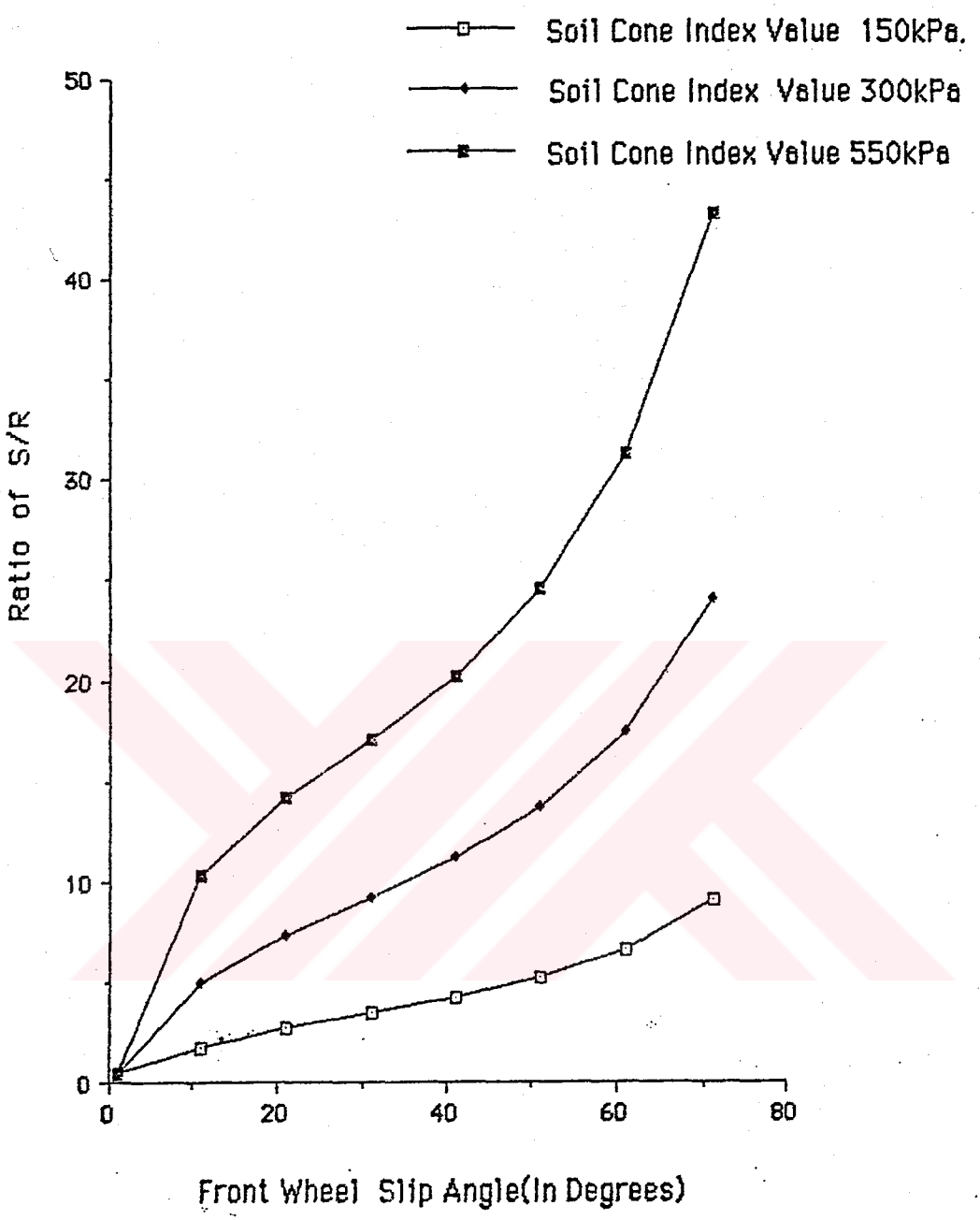

Figure 4.7 The Ratio of Steering Forces and Rolling Ressistance for Various Front Wheel Slip Angle .

CHAPTER V

PRELIMINARY DESIGN OF IRON-WHEEL

5.1 Introduction

As was shown in the previous chapters, small tractors fitted with pneumatic tyres are not capable of developing the required drawbar pull for primary cultivation in arid and semi-arid regions. This was shown clearly to be so in Chapter IV for Başak-17 tractor. Even the drawbar pull required for secondary cultivation is developed at fairly high wheel slip so the resulting tractive efficiency is usually low. This results in power losses in small tractors amounting to more than half of the tractors engine power output. Thus a solution should be to so that the small tractors can develop high tractive efficiency and achieve high engine power utilization.

The solution proposed in this thesis is the use of a rigid wheel with lugs. Such a wheel could be used in place of pneumatic tyre and it will be henceforth the termed as an Iron-Wheel.

Such wheels have been extensively used in rice growing countries of Asia. However due to the difference in soil conditions, their design concept (or requirement) are markedly different from

the one developed in this thesis [25].

Iron wheels used in paddly field are designed to have good tractive and floating performance [25] and these requirements influence the overall design procedure. In some cases the Iron Wheels are designed to have easy sinkage so that the lug tips would be able to catch the comparatively hard layer under the loose flooded surface soil to assist in traction [26]. Two most commonly used Iron-Wheel configurations for paddy fields are shown in Figures. 5.1 (a) shows open lug wheels for two wheel power tillers where avarage weight and power is 200-300 kg and 7.0 kw respectively. (b) shows an example of Iron-Wheel used with tractor tyres as an auxillary device [26].

From the above discussion is quite clear that the performance requirements of Iron-Wheel for paddy region is quite different from those for arid region and therefore a rational design procedure should be developed and expected performance predicted.

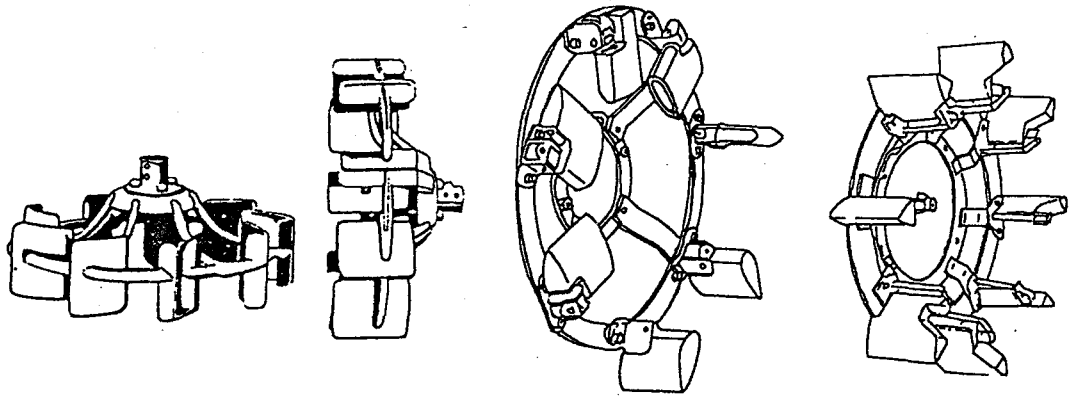

(a) (b)

Figure 5.1 Lug Wheels Used in Puddy Region

(a) Open Lug Wheel (b) Float Type Lug Wheel.

The first step in developing the design procedure is studying the modes of interactions of lug-soil system in the Iron-Wheel. Two principle methods for modelling lug-soil interaction will be studied and these are

(i) slip line field theory

(ii) Rankine passive earth pressure theory

The basic assumptions of both theories are the following [27, 28]:

(i) soil failure takes place in a two dimensional field.

(ii) the soil is an isotropic, rigid-plastic material which fails at zero strain according to mohr-coulomb criterion according to the effective stress relationship given by

$$\tau_f = C + \sigma_t \tan \theta . \qquad (5.1)$$

(iii) The shear stress mobilized on the soil structure-interface can be described by effective stress relationship

$$\tau_f = a + \sigma_f \tan \gamma \qquad (5.2)$$

(iv) The deformation takes place slowly and inertia forces ignored [29]

The use of the slip line field theory for prediction of forces at soil lug interface gives a good correlation with experimental values particularly for sandy soils. However the calculated values using the theory underestimates the forces at soil-lug interface for silty loam soil [30, 31]. Actually the slip line field theory could be used to model the soil-lug interactions very accurately for sandy soil and the like;

but for majority of soil found on off-road conditions the theory does not offer an accurate solution [28]. An analysis by Tomio et al. [30] using slip line field theory will be included in this thesis to offer a wider picture of the existing methods for modelling lug-soil interaction and hoping that more refinement would be made on the theory rendering it more useful for prediction of forces at the soil-lug interface.

The Rankine passive earth pressure-theory will be used for modelling the lug soil interaction in this study mainly because it has been tried and found to give good correlation with experimental results, both in prediction of force acting on lug [32, 33] and rigid tines [34]. A more detailed explanation of this theory will be given later in the Chapter.

5.2 Use of Slip Line Field Theory for Modelling Soil-lug Interaction

There have been widespread attempts to model the soil behaviour under the action of lug by means of theory of plasticity. Earliest detailed work was reported by Bekker [33] where he conducted a theoretical analysis on a slip line developed by rear most shoe of the track by using theory of plasticity. Nowatzki et al. [35] used the same theory to find the mode of interaction between a rigid driven wheel and the sand medium it was driven on. The method explained here was developed by Tomio et al [30] and the method is as follows.

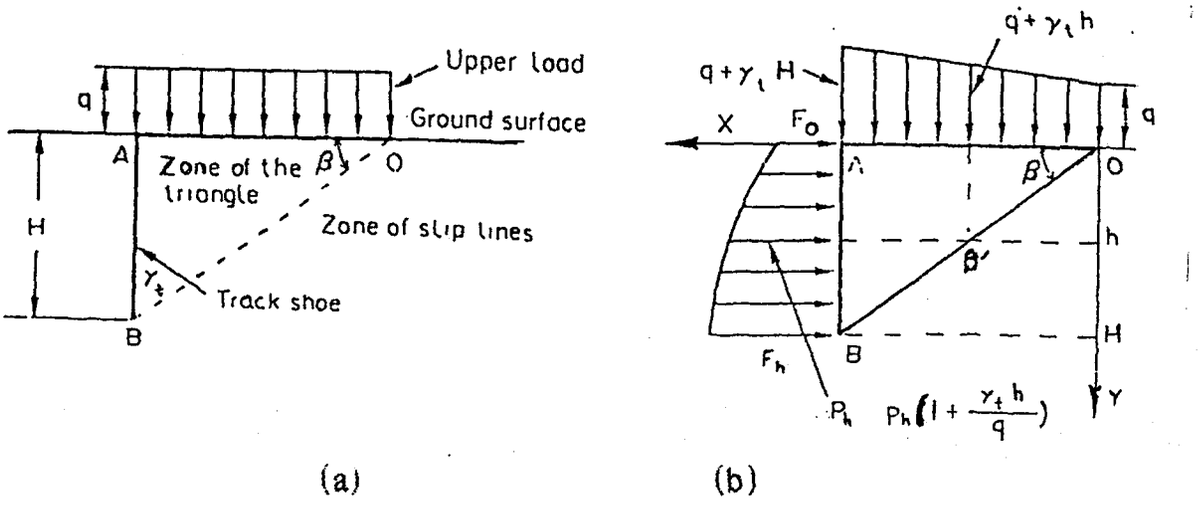

Figure 5.2 (a) Cross section of a Track Shoe (b) Schematic Diagram of Track Shoe Showing Forces

The Figure 5.2 represents a cross section of a track shoe. The line OB shown in Figure 5.2 (a) will be termed as the boundary line. The area enclosed by the boundary line and the track shoe is termed 'the zone of the triangle' It is assumed that the slip lines are be developed in the zone below the boundary line OB. The thrust ΔF is developed by the resistance to slip along a differential slip line and the overall thrust ΔF would be obtained by intergrating DF along the entire boundary line OB.

5.2.1 Forces in the Zone of the Triangle

The forces acting on the triangle zone of are the distributed load, q, acting on the plate AB and the soil weight above the boundary line. By using theory of plasticity, the shearing force

acting along a slip line can be found. If the thrust force due to the distributed load q is P_h at point B' the thrust due to $q + y_t h$ would be $P_h (1 + y_t hq)$

After obtaining the relationship between the vertical force and thrust force at point B from Figure 5.3. Mohr circle is drawn for point B. This circle passes through point (σ, τ), which was obtained from Figure 5.3 and is tangent line of a soil having cohession, c and angle of internal friction, ϕ. Once the circle is drawn σ_n and ψ can be obtained, where σ_n is the major principle stress and ψ the angle between the direction of σ_n and the normal line on the boundary line OB at point B'

Figure 5.4 shows the Mohr's circle from which σ_n and ψ can be obtained from the Figure 5.3 and 5.4. σ_n and t at the point B' are obtained as

$$\delta_n = \tau \tan \beta + q + yt\, h$$

$$\tau = \frac{1}{2} \{ ph (1 + y_t . h/q) - (q + y_t h) \} \text{Sin } 2\beta \qquad (5.1)$$

$$\delta_n = Ah + Bh \text{ Cos } 2\phi$$

$$\tau = Bh \sin 2\phi \qquad (5.2)$$

where

$$\left.\begin{matrix} A_h \\ B_h \end{matrix}\right\} = \frac{\delta_h}{2} \{ 1 + \tan^2 (\frac{\pi}{4} - \phi/2) \} \pm c \tan (\frac{\pi}{4} - \phi/2).$$

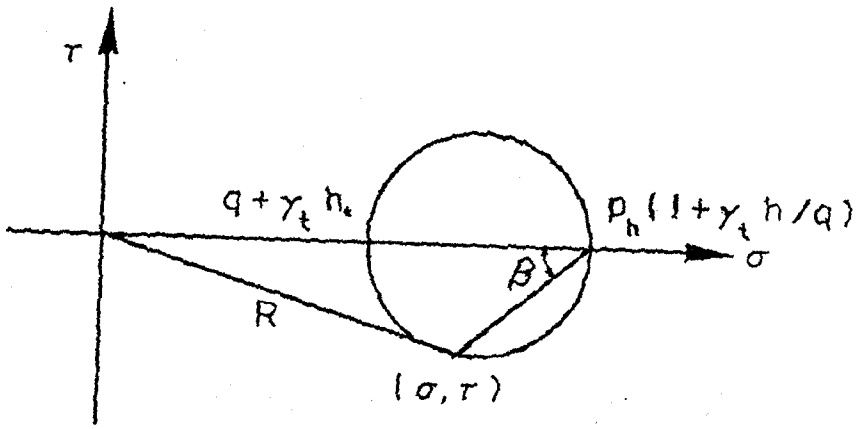

Figure 5.3 Relationship Among the Unit Forces at Point B' in Figure 5.2

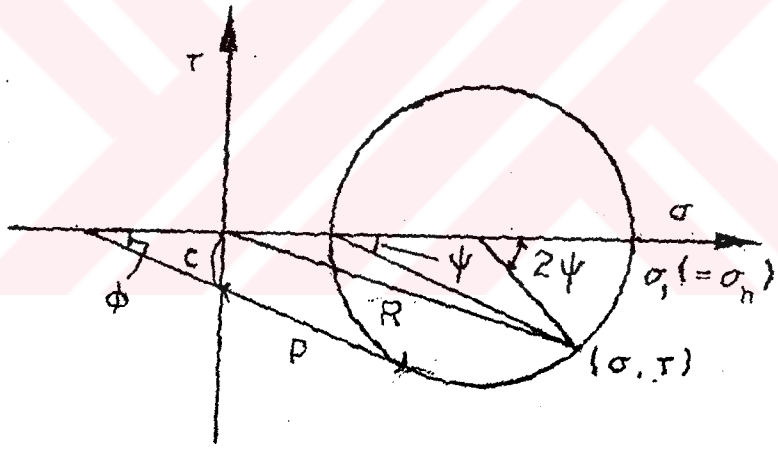

Figure 5.4 Stress Circle at a Boundary Point B' Between Triangle OAB and the Ground.

Substituting equation (5.2) in to the first part of equation (5.1). Thus equation below is obtained.

$$Ah + Bh \cos 2\psi = Bh \sin 2\psi \tan \beta + q + y_t h \qquad (5.3)$$

The above equation is the first the equations needed to obtain the values of σ_n and ψ.

Analysis of slip lines and stress in the zone of slip lines. The zone of slip lines will be divided in to three zones as shown in Figure 5.5 which are assumed to exibit completely different behaviours and these are

(i) zone of active state

(ii) zone of plastic state

(iii) zone of passive state.

The shape of slip lines in these three zones and shearing resistance force along these lines are obtained by using the theory of plasticity.

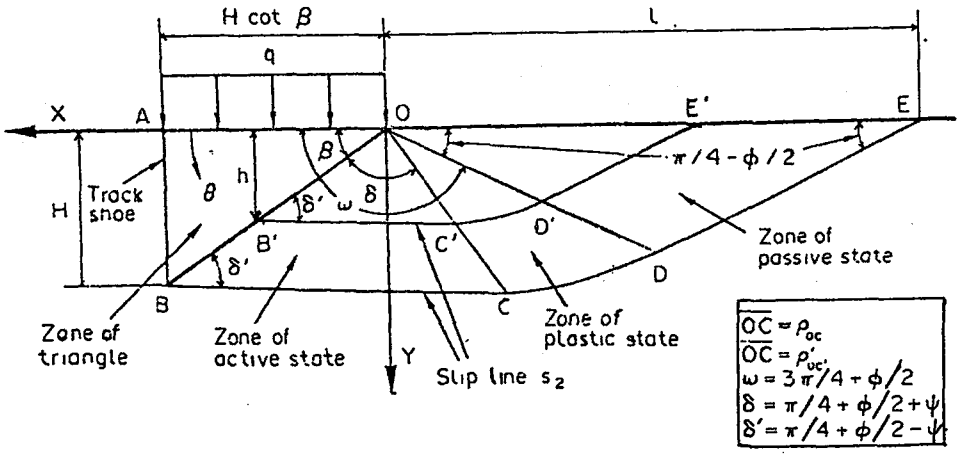

Figure 5.5 General Diagram for Analysis

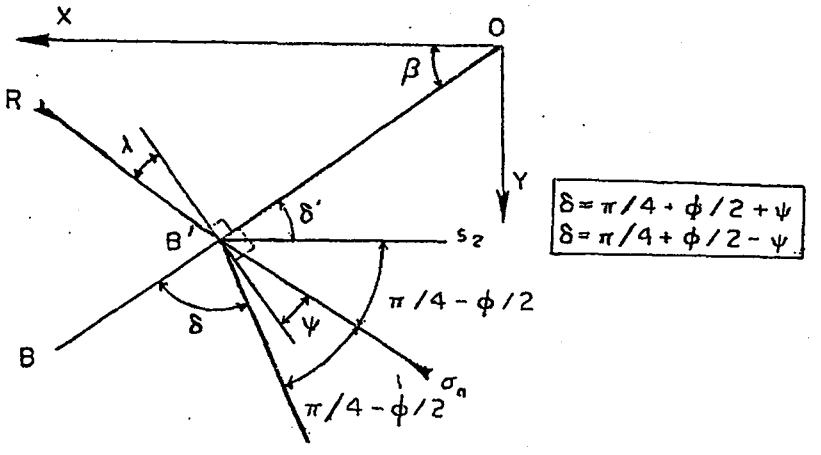

Figure 5.6. Slip Lines Against the Boundary Line OB at a Point B'

5.2.2 The Zone of Active State

The angle between the slip line S_1 and the x-axis is given as follows.

$$\theta = \frac{\pi}{4} + \frac{\phi}{2} + \psi + \beta \qquad (5.4)$$

The stress P on the slip line S_2 should satisfy the following equation

$$\frac{\partial p}{\partial s_2} + 2\left(p \tan\phi + \frac{c}{\cos\phi}\right)\frac{\partial \theta}{\partial s_2} = \gamma_t \cos\theta \qquad (5.5)$$

Since the slip line S_2 is a straight line, integration of equation (5.5) they gives

$$p = y_t \cdot S_2 \cos\theta + k_1 \qquad (5.6)$$

The integration constant k_1 is obtained by refering to the point B' where $S_2 = 0$ and PB' is known.

$$PB = \sigma_h \tan(\pi/4 - \phi/2) - c \qquad (5.7)$$

Substituting PB into equation (5.6), the following result is obtained

$$p = y_t S_2 \cos q + \delta_n \tan(\pi/4 - \phi/2) - c \qquad (5.8)$$

5.2.3 The Zone of Plastic State

The slip lines S1 in the zone of plastic state OCD, in Figure 5.5 is considered to be one of the radial lines which have their origin at point 0. Slip line S2 is considered to be a logarithmic spiral. However the equations of the yield condition of soil are generally given as follows [30]

$$\begin{aligned} \sigma_x &= \sigma_m (1 + \sin\phi \cos 2\alpha) + C \cos\phi \cos 2\alpha \\ \sigma_y &= \sigma_m (1 - \sin\phi \cos 2\alpha) - C \cos\phi \cos 2\alpha \\ \tau &= (\sigma_m \sin\phi + C \cos\phi) \sin 2\alpha \end{aligned} \qquad (5.9)$$

where

$$\sigma_m = \frac{1}{2}(\sigma_1 + \sigma_1) \text{ and } \alpha = \theta + \frac{\pi}{4}\theta/2 \qquad (5.10)$$

Also, the equations of equilibrium are represented as follows.

$$\frac{\partial \sigma_x}{\partial x} + \frac{\partial \tau}{\partial y} = 0 \quad \text{and} \quad \frac{\partial \sigma_y}{\partial y} + \frac{\partial \tau}{\partial x} = \gamma_t \tag{5.11}$$

Substituting equation (5.7) into equation (5.8), the equation for characteristic slip line is obtained as

$$L_n \rho' = \theta \tan \phi + k_2 \tag{5.12}$$

where ρ' is the length of the radius on the slip line S_2 and K_2 is the integration constant. In order to obtain value of k_2 we use the boundary condition of $\rho' = \rho'_{OC}$ at the point C'. As can be seen from Figure 5.5, θ will became $(\beta + \delta)$ at point C'. ρ'_{OC} in the zone of active state is given follows

$$\rho'_{OC} = h \operatorname{cosec} \beta \sec \phi \sin \delta' \tag{5.13}$$

Substituting equation (5.13) q = b + d in to equation (5.12), r' is

$$\rho' = \rho'_{OC} \exp [(\theta - \delta - \beta) \tan \phi] . \tag{5.14}$$

The stress p, on the slip line S_2, is now obtained by substituting equation (5.14) into equation (5.5).

$$\frac{dp}{d\theta} + 2p \tan \phi = \gamma_t \rho'_{OC} \exp [\theta - \delta - \beta) \tan \phi] \cos \theta \sec \phi - 2c \sec \phi \tag{5.15}$$

integrating the above equation, the stress p, on the slip line S_2 found to be

$$p = \frac{y_t \rho'_{OC} \exp[(\theta - \delta - \beta)\tan\theta] \sec\phi (\sin\theta + 3\tan\theta\cos\theta) - c\,\mathrm{Cosec}\,\phi}{1 + 9\tan^2\phi}$$

$$+ k_3 \exp[-2q \tan f] \qquad (5.16)$$

where k_3 is the integration constant

5.2.4 The Zone of Passive State

The slip lines in the zone of passive state consist of straight lines S_1 and S_2 which intersect at equal angles. From equation (5.5), the stress P, on the slip line S_2, is given as follows

$$p = y_t S_2 \cos\theta + k4 \qquad (5.17)$$

where k_4 is the integration constant from Figure 5.7, the value of k_4 is known to be C. Hence, equation (5.17) becomes

$$p = y_t S_2 \cos\theta + C \qquad (5.18)$$

5.2.5 Relationship of the Stresses Among the Three Zones

The major principal stress at point B' in figure 5.5 can be determined by connecting the stresses among the zones of active state, plastic state and passive state.

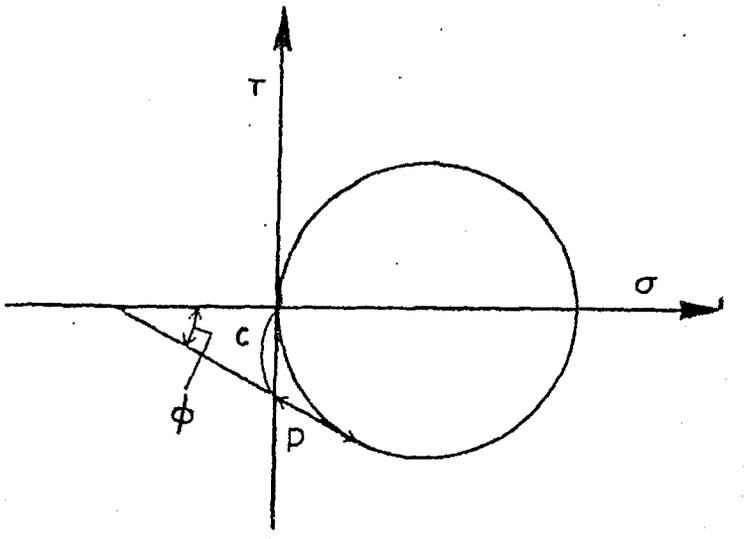

Figure 5.7 Relationship Among the Stresses at the Ground Surface In the Zone of Passive State.

First consider the continuous condition of stress at the point D' between the zone of passive state and zone of plastic state in figure 5.5. then, θ and S_2 are given as follows

$$\theta = -(\pi/4 - \phi/2) \text{ and } S_2 = D'E' \qquad (5.19)$$

Substituting these relations into equation (5.18), the stress P_D', at point D', is given by the following equation

$$P_D' = \gamma_t \, D'E' \cos(\pi/4 - \phi/2) + C \qquad (5.20)$$

As is clear from figure5.5 that D'E', in the above equation is equivalent to OD' which is the radius at point D' in the zone of plastic state. From equation (5.14) the length of OD' is given by

$$OD' = \rho'_{OC} \exp[(\pi/2 - \beta - \phi)\tan\phi] \quad (= D'E'). \qquad (5.21)$$

Therefore substituting this equation into equation (5.20), P_D becomes

$$P'_D = \gamma_t \cdot \rho'_{OC} \exp [(\pi/2 - \beta - \psi) \tan \phi] \cos ((\pi/4 - \phi/2) + C \quad (5.22)$$

On the other hand, stress PD at point D' in the zone of plastic state is obtained by substituting $\theta = \omega\ (3\ \pi/4 + \phi/2\ )$ in figure 5.5 into equation, is naturally equal to stress P_D , in the zone of passive state which is obtained by equation (5.22). As a result, the integration constant k_3, in equation (5.16) is obtained. Therefore, stress P in the zone of plastic state is given by the following equation

$$P - \gamma_t \rho'_{OC'} [\exp [(3\omega - 2\theta - \delta - \beta) \tan\theta] \cos (\frac{\pi}{4} - \frac{\phi}{2}) + \frac{\text{Sec}\,\phi}{1 + 4 \tan^2 \theta}$$

$$(\sin \theta + 3 \tan \phi \cos \theta) \exp [(\theta - \delta - \beta) \tan \phi] - (\text{Sin}\ \omega + 3 \tan \theta \cos \omega) \exp [3\omega - 2\theta - \delta - \beta) \tan \phi] + \{ (1 + \sin \theta \exp [2 (\omega - \theta) \tan \phi] - 1) c \operatorname{cosec} \phi . \quad (5.23)$$

Next, consider the continuous condition of stress at point C (figure 5.5) on the boundary line between the zone of plastic state and the zone of active state. First the stress at point C' in the zone of plastic state of must be obtained, By substituting $\theta = \delta + \beta$ into equation (5.23) as follows

$$P'_C = \mu_1\ \rho'_{OC} [\exp [3 (\omega - \delta - \beta \tan \theta] \cos (\frac{\pi}{4} - \phi/2) + \frac{\sec\phi}{1 + 9}$$

$$(\sin (\delta + \beta) + 3 \tan \phi \cos (\delta + \beta) - (\sin \omega + 3 \tan \phi \cos \omega) \exp [3 (\omega - \delta - \beta) \tan \phi])] + \{ (1 + \sin \phi) \exp [2 (\omega - \delta - \beta) \tan \phi] - 1 \} \operatorname{cosec} \phi . \quad (5.24)$$

Also. P_C' in the zone of active state may be obtained by

substituting $\theta = \delta + \beta$ and $S_2 \rho_{OC} \sin \delta / \cos(\delta - \phi)$ in figure 5.5 into equation (5.8)

$$P'_C = \frac{\gamma_t \rho'_{OC} \sin \delta \cos(\delta + \beta)}{\cos(\delta + \phi)} + \delta_h \tan(\pi/4 - \phi/2) - C \qquad (5.25)$$

However, the values of P_C' evaluated by the above equation should be equal to value evaluated by equation (5.24). Therefore the major principle stress δ_n is given as

$$\sigma_n = \tan\left(\frac{p}{4} - \frac{\phi}{2}\right)\left(P'_C + C - \frac{\mu t \rho_{OC}' \sin \delta \cos / (\delta+\beta)}{\cos(\delta-\phi)}\right) \qquad (5.26)$$

where PC' is the value evaluated by equation (5.24)

5.2.6 Calculation of Thrust

The thrust exerted by a grouser is obtained by the following approach. First the unknown quantities σ_h and ψ are calculated from equation (5.26) and (5.3) and then τ is calculated by substituting these values in equation (5.2). Next, substituting the value of τ in to the second part of equation (5.1), the unit P_h may be obtained by the following equation

$$P_h = q \frac{(2\,Bh \sin 2\psi \ \mathrm{cosec}\, 2\beta + q + y_t + h)}{q + y_t h} \qquad (5.27)$$

Therefore, the thrust at point B' in figure 5.5 is found by substituting this value Ph into $Ph\,(1 + y_t\, h/q)$ shown in Figure (5.1).

Thus, the total thrust F, exerted by grouser. AB is obtained by integrating ph $(1+y_t h/q)$ along the boundary line OB

$$F = \int_0^H Ph\,(\,1 + q_t h/q\,)\,dh \quad N/m \tag{5.28}$$

5.3 Modelling of Lug-Soil Interaction by the Use of Passive Earth Pressure Theory

5.3.1 Introduction

There exists a close analogy between the modes of failure encountered in long retaining walls and track laying tractor running gear [36-38]. This analogy is not limited to the actual physical similarity between this structures but extension to more significant factors associated with the modes of soil failures and actual failure surface geometry involved [29]. Thus the same theoretical analysis can be applied to explain the modes of soil failure encountered in both long retaining walls and tractor runing gear.

Passive earth pressure theory, which has long been used by civil engineers to analyse the modes of soil failure encountered in long retaining walls and strip footings will be used in this section to model the lug-soil interaction. A detailed explanation of the modelling process is as follows.

In general the soil load L required to cause failure on a plane loaded interface can be expressed in terms of the following variables

$$L = f (y, \phi, C, \delta, Ca, Z, q) \qquad (5.29)$$

By means of dimensional analysis, equation (5.29) can be written more specifically in terms of the dimensionless groups

$$L/ y_Z2 = f (C/_{yZ} , Ca/ yZ , q/ yZ , \phi, C, \delta, \alpha) \qquad (5.30)$$

Reece [29] proposed that equation (5.30) could be written in the form of the additive equation below

$$L = y_Z^2 N_y + C_c Z N_C + C_a Z Na + q Z N_q \qquad (5.31)$$

The four terms of equation (5.31) represent, gravitational, cohesive, adhesive and surcharge components of the soil reaction per unit width of the interface. The Reece factors Na , Nc , Na and Nq represent the shape of the soil failure boundry and are thus a function of ϕ, δ, and the geometry of the loaded interface.

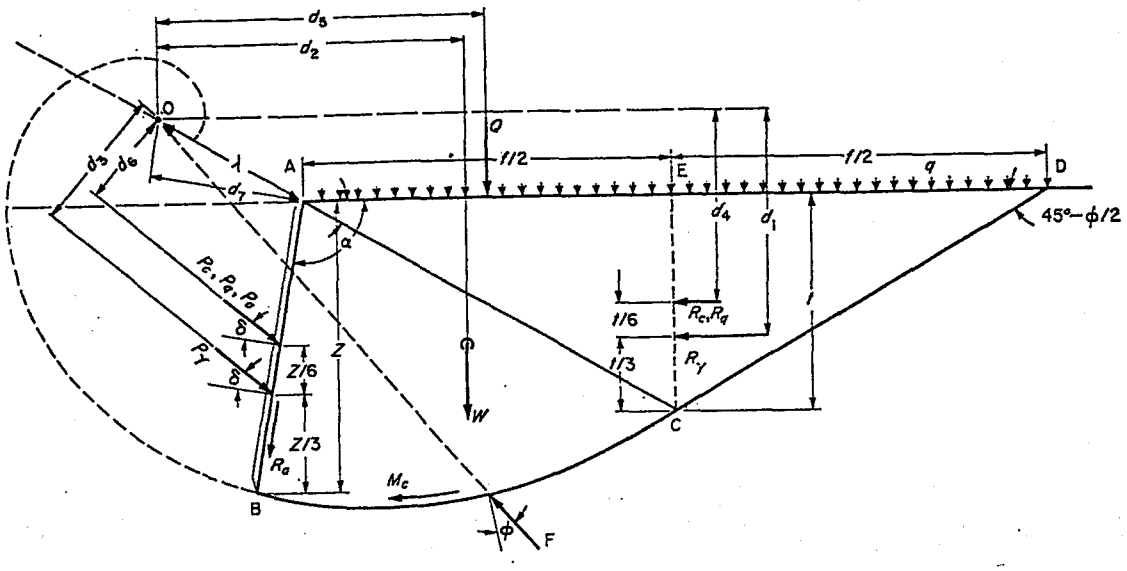

Figure 5.8 Diagram Showing Logarithmic Spiral Failure Boundary and The Directions of Various Forces Acting On the Soil Interface Boundary [28].

Hettiaratchi et al [29] produced charts from which the values of the N-factors for various δ ϕ and α (see Figure 5.8) could be found. Another important chart produced by the same authors were for determining the rupture distance AD shown in Figure 5.8. The error resulting from using this method for obtaining passive earth pressure value for two dimensional soil failure problems was shown to be negligible for must practical purpose [29].

This method should not be used for prediction of forces at soil interface for wet clay soils as the mode of soil failure boundary is quite different from the one assumed by conventional soil mechanics [39, 40]. The force predicted by this theory was, naturally found not to

correlate experimental results for wet clay soil [31]. Passive earth pressure theory should be used to predict forces in soil-lug interaction for a purely frictional, a purely cohessive and a c-ϕ type of soil as the mode of failure and failure boundary for these soils are the same as that assumed by the theory [29]

5.3.2 Mathematical Modelling of a Single Lug

The basis for modelling the soil-lug interaction would be equation (5.31) written below

$$L = \gamma Z_c^2 N_\gamma + CN_c Z_c + C_a Na Z_c + qN_q Z_c \qquad (5.31)$$

Refering back to Figure 5.8 the force L would be acting at an angle δ to the normal of the interface. The angle of interface to the horizontal is α. Therefore the horizontal component of force L would be given by

$$L_H = L \cos (\alpha + \delta - \pi/2) + C_a Z_c \cos \alpha \cos (\pi - \alpha) \qquad (5.32)$$

$$L_H = L \sin (\alpha + \delta) - C_a Z_c \cos^2 \alpha. \qquad (5.33)$$

The lug's vertical depth. Z_c in given by

$$Z_c = Z \cos (\pi/2 - \alpha) = Z \sin \alpha \qquad (5.34)$$

where

Z_c : Interface depth or lug depth

Z : Interface length

The term $C_a Z\cos\alpha$ arises from frictional forces acting on the soil failure surface due to adhesive forces along the interface and is additional to the actual adhesion. Equation (5.34) is the first step toward modelling the performance of iron wheel.

5.3.3 Lug Displacement Equations

In this section displacement equations for a single lug moving through a soil medium will be derived. Figure 5.9 shows a schematic diagram of an Iron-Wheel where of all the angular relationships required to derive the displacement equation are shown. For the sake of simplicity, the co-ordinate system is defined as given in the figure and angle λ is measured counter-clockwise between the x-axis and the line OS. As the lug is represented in the diagram as a line segment PS, the description of the displacement of points P and S would be enough to describe the lug's displacement. Therefore the lug displacement equation could be written in terms of displacement of points P and S.

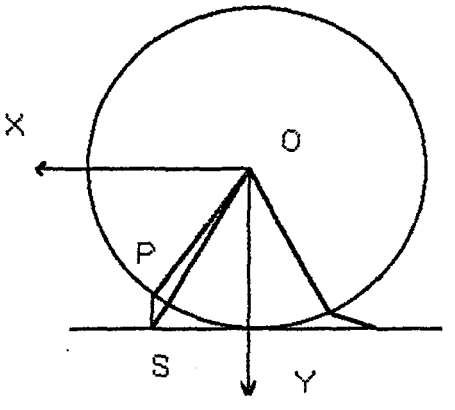

Where

$<XOP = \lambda_f$

$<POS = \phi_i$

$<POY = \phi_L$

$OP = r_1$

$OS = r_2$

$PS = Z$

Figure 5.9 A Sketch of Iron-wheel Showing the Relationship of Various angles

For a stationary Iron-Wheel rotating about point 0 as shown in the diagram, the co-ordinates of point P and S are

$$\begin{aligned} P_x &= r_1 \cos(\lambda + \phi_i) \\ P_y &= r_1 \sin(\lambda + \phi_i) \\ S_x &= r_2 \cos \lambda \\ S_y &= r_2 \sin \lambda \end{aligned} \qquad (5.35)$$

where

r_1 : Radius of the Iron-Wheel

P_x , S_x : x-co-ordinate of points P and S respectively.

P_y , S_y : y-co-ordinate of points P and S respectively.

and

$$\phi_i = \tan^{-1}\left[\frac{\sin\beta}{r/z + \cos\beta}\right] \qquad (5.36)$$

$$r_2 = \frac{z\sin\beta}{\sin\phi_i} \qquad (5.37)$$

where b : Lug inclination angle as shown in the diagram

Z : Lug's length

Since displacement of the lug through a soil medium is of importance to this study, the displacement equations of the lug would be derived for lugs in contact with soil or in otherwords for lugs whose angle λ is such that $\lambda_f < \lambda < \lambda_L$, whereby the values of λ_f and λ_L are given by the equations below.

$$\lambda_f = \pi/2 - \phi_L$$
$$\lambda_L = \pi/2 + \phi_L \qquad (5.38)$$

The value of the angle ϕ_L is obtained from equation (5.39)

$$\phi_L = \cos^{-1}(r_1 / r_2) \qquad (5.39)$$

The co-ordinates of points P and S for a rolling Iron-Wheel with a wheel slip s is given by the equations below.

$$P_x = (\lambda - \lambda_f) . r_1 (1 - s) + r_1 \cos(\lambda - \phi_i),$$
$$P_y = r_1 \sin(\lambda - \phi_i) \qquad (5.40)$$
$$S_x = (\lambda - \lambda_f) . r_1 (1-s) + r_2 \cos\lambda$$
$$S_y = r_2 \sin\lambda$$

By using equation (5.40) the motion of a lug through the soil medium can be simulated. These equations would be helpful in understanding and modelling the soil-lug interaction.

5.3.4 Modelling the Compressibility of the Soil

The majority of soil found in off-road conditions and particularly agricultural soil have a high degree of compressibility [28]. Thus any modelling of soil-lug interaction without taking the soil's compressibility into account would be incomplete and would certainly lead to inaccurate results. Experiments by Gee-clough et al [40] showed that the forces required to cause soil-failure at the soil interface could be predicted quite closely by Equation (5.31) though the soil displayed a degree of compressibility. In other words, equation (5.31) could the used to predict the force required to cause failure of the soil at the soil-interface boundary, but the variation of forces at the soil-interface with the interface's lateral diplacement would be modelled by using experimental results obtained by Gee clough et al [40]. Figure 5.10 shows the variation of forces at soil-interface boundary with interface lateral displacement. The forces increase almost linearly with lateral displacement of interface until the soil failure occurs, whereby the forces start decreasing abruptly

just to rise again to a new peak, and the cycle repeats.

Studies in civil engineering have shown that lateral displacement of long retaining walls required to cause failure at the soil-wall boundary is related to the depth of the wall in the soil by equation (5.41) [33]

$$K_w = L_w / Z_w \quad (5.41)$$

where

L_w : wall's lateral displacement.

Z_w : wall's depth in the soil.

K_w : aconstant depending on the soil type and soil condition.

Due to the great analogy between long retaining walls and Iron-Wheel lugs (see section 5.31), it will be safe to assume that the ratio of the lug's lateral displacement to lug's depth in soil is constant for a particular soil type or condition and the variation of the forces at the lug-soil interface with lug's lateral displacement is represent by Figure 5.10.

The soil compressibility will be modelled by idealized the variation of the force experienced at the soil-lug interface as shown in Figure 5.11 by:

(i) Replacing the lug's lateral displacement in Figure 5.10 by a ratio of lug's lateral displacement to lug's depth in soil as given by equation (5.42) below

$$e = l / Z \qquad (5.42)$$

where l : lug's lateral displacement.

Z : lug's depth in soil.

e : a non-dimensional parameter.

(ii) Replacing the variable force in Figure 5.10 by a ratio of the variable force to the force required to cause soil failure at the soil-lug interface as represented by equation (5.43) below

$$P = L_V / L_H \qquad (5.43)$$

where

L_V : The variable force experienced at the soil-lug interface

L_H : The force required to cause soil-failure at the soil-lug interface

P : Soil compressibility correction factor

(iii) Assuming a linear variation between the force at the soil-lug interface and the lug's lateral displacement before failure and by replacing the cylic force after soil failure as shown in Figure 5.10 by a constant force.

The equations to be used to model the soil's compressibility can be derived from figure 5.11 and are given as

$$\left.\begin{array}{ll} P = 1.428\ e & \text{for} \quad 0 \le e \le 0.7 \\ P = 1 & \text{for} \quad e > 0.7 \end{array}\right\} \qquad (5.44)$$

Due to similarity of the soil conditions found in arid and semi-arid regions and of that used by Cle-clough et al [40] to obtain Figure 5.10, the equations derived above will be used to model the soil's compressibility in arid and semi-arid regions. To model the compressibility of other soil types, experiments should be performed to obtain the variation of the force at the soil-interface boundary with lateral displacement similar to that shown in Figure 5.10.

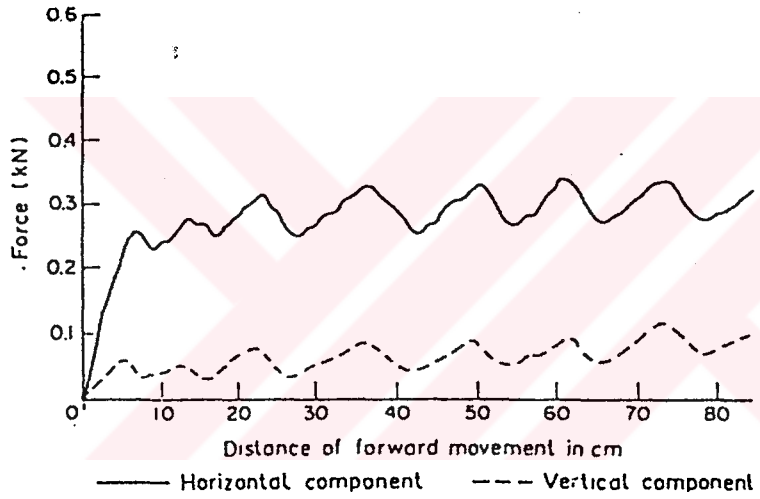

Figure 5.10. The Variation of load Required to Cause Failure at Boundary with Displacement

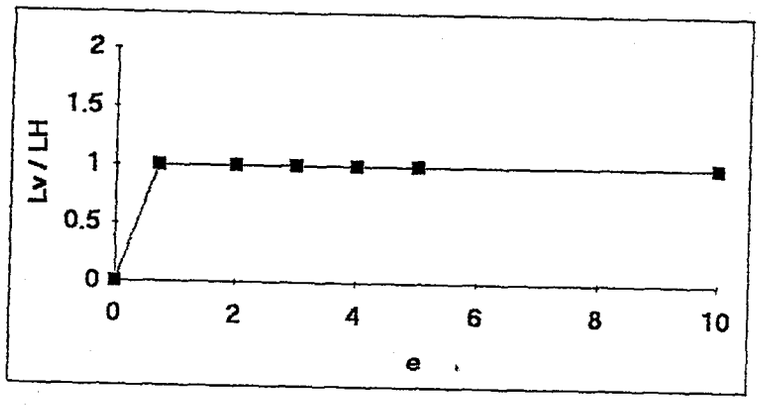

Figure 5.11. The Idealized Variation of load Required to Cause Failure at Boundary with Displacement

In case the drawbar pull contribution of each lug in contact with the soil is to be calculated, the soil compressibility correction factor p for a lug at any position in the Iron-Wheel has to be derived. In section 5.3.3 it was shown that the angle, λ, given in Figure 5.9 is very convinient to derive the lug's displacement equations and will be used to derive a relationship to enable the calculation of the soil compressibility correction factor P of a lug at any lug position.

For a rotating Iron-Wheel the lug's lateral displacement l_i is

$$l = \frac{1}{2}\left[r_1 \cos(\lambda_f - \theta_i) + r_1 \cos\lambda_f - (2 r_1 (\lambda - \lambda_f)(1-s) + r_2 \cos\lambda \right.$$

$$\left. + r_1 \cos(\lambda_f - \phi_i)) \right] \qquad (5.45)$$

the lug's depth at any angle λ is given as

$$Z_c = r_2 \sin\lambda - r2 \sin\lambda_f - Zin$$

$$e = l/Z_c \qquad (5.42)$$

$$P = 1.428\ e = 1/Z_c \qquad \text{for } 0 \leq e \leq 0.7 \qquad (5.46)$$

$$P = 1 \qquad \text{for } e > 0.7 \qquad (5.47)$$

The equations derived above will be used to model the soil's compressibility and will enhance the accuracy of the modelling of the soil-lug interaction given in this thesis.

5.3.5 Prediction of Drawbar Pull Due to Iron-Wheel Lugs

After having derived the lug's displacement equations and modelled the compressibility of the soil, the next step will be to derive an equation from which the drawbar pull that can be achieved with an Iron-Wheel with lugs in contact with soil could be predicted. Though the development of a criterion for optimum spacing of Iron-Wheel lugs will be done later in this chapter, it will be assumed here that more than one lug is in contact with the soil at any particular time.

Figure 5.12 shows a schematic diagram of a rotation Iron-Wheel showing various parameters required to derive the drawbar pull from Iron-Wheel lugs in contact with soil.

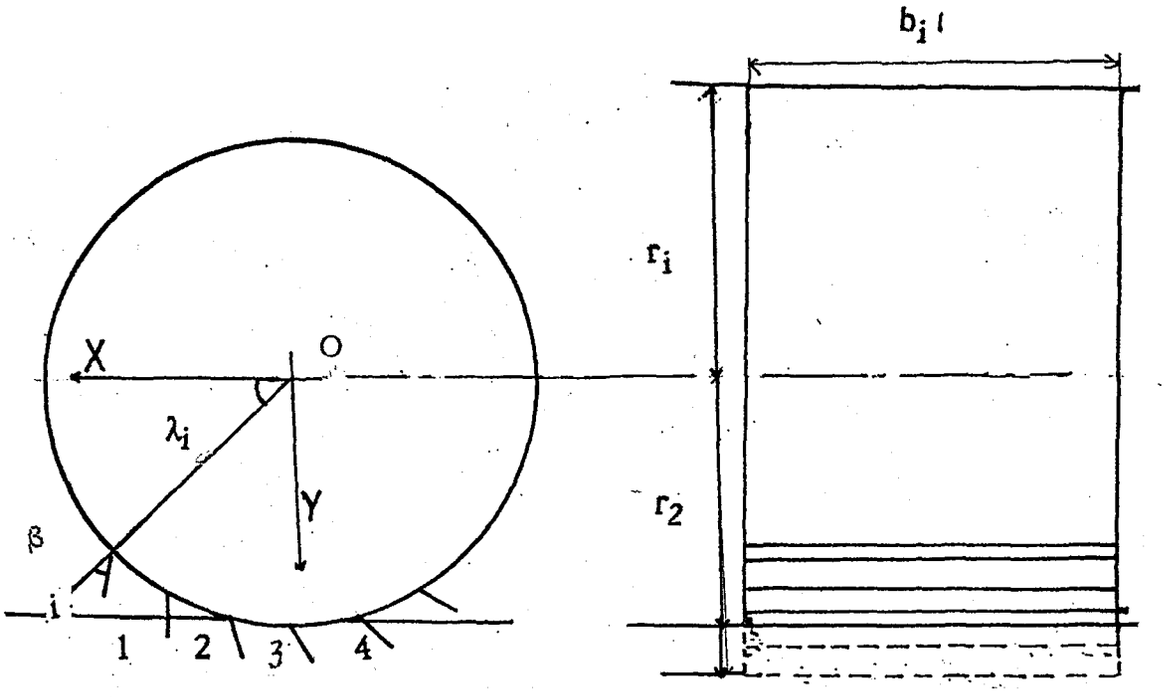

Figure 5.12 Schematic Diagram of a Rotating Iron Wheel

The maximum horizontal force per unit lug width required to cause soil-failure in the lug-soil interface is given by equation (5.33)

$$L_H = L \text{ Sin } (\alpha + \delta) - Ca\ Z_c \text{ Cos}^2 \alpha \qquad (5.33)$$

where L is given by equation (5.31)

$$L = y\ Z^2\ N_y + Ca\ Z\ Na + C_c\ N_c\ Z + q\ N_q\ Z \qquad (5.31)$$

By using the relationship given in equation (5.48) , the angle α in equation (5.33) can be substituted by λ and β as given in equation (5.49)

$$\alpha = \pi - \lambda - \beta \qquad (5.48)$$

$$L_H = L \sin(\pi - \lambda - \beta + \delta) - Ca\, Z_c \cos^2(\pi - \lambda - \beta) \qquad (5.49)$$

Simplifying equation (5.49) gives

$$L_H = L \sin(\lambda + \beta - \delta) - Ca\, Z_c \cos^2(\lambda + \beta)$$

By multiplying equation (5.50) by the soil compressibility factor, P and the lug width, b_i , the horizontal force experienced at lug-soil interface and thus the lugs contribution to the drawbar pull is found as given by equation (5.51).

$$T = b_i P [L \sin(\lambda + \beta - \delta) - Ca\, Z_i \cos^2 (\lambda + \beta)] \qquad (5.51)$$

where

T : Horizontal force experienced at lug-soil interface

The drawbar pull from Iron-Wheel lugs is given by the summation of the contributions from all the lugs in contact with soil and is given as

$$T_i = \sum_{i=1}^{N_Z} b_i [P_i l_i \sin(\lambda_i + \beta - \delta) - Ca\, Z_i \cos(\lambda_i + \beta)] \qquad (5.52)$$

where

Z_i : Instantaneous depth of each lug given by the equation below

$$Z_i = r_2 \sin \lambda_i - r_2 \sin \lambda_f - Z_{in}$$

L_i : Maximum force required to cause soil failure at the soil

interface boundary for the instantaneous lug depth for each lug given by equation below

$$L_i = y Z_s^2 Ny_i + N_{ci} C_c Z_s + N_{qi} Z_s q + Na_i Z_s Ca \qquad (5.54)$$

N_{yi} , N_{ci} , N_{ai} , N_{qi} : Reece factors for each lug.

N_z : Total number of lugs in contact with soil.

P_i : Compressibilty correction factor for each lug.

b_i : Iron-wheel width.

By using the equations above the drawbar pull the from Iron-Wheels lugs can be predicted.

5.3.6 Contribution of the Unlugged Area of the Iron-wheel in Contact With Soil to Drawbar Pull

When a driving wheel rotates on a typical exposed soil it causes the soil underneath the wheel to deform horizontally. Actually the resistance of the soil to the shearing action of the soil top layers by wheel as it tries to pull the vehicle load is what translates to the wheel's drawbar pull. In other words, the drawbar pull from the vehicle's driving wheels equals to the force required to cause the horizontal deformation of the soil top layer. Therefore the drive wheel's drawbar pull can be predicted by determing the force required to deform a soil top layer by a particular ammount horizontally.

Janosi and Hanomoto [41] proposed an equation for describing the soil shear curve and it will be the basis for developing an equation for predicting the drawbar pull of the unlugged area in contact with soil. The equation proposed by Jonasi and Hanomoto is as follows

$$\tau = \tau_m (1 - \exp (\Delta/k)) \qquad 5.55$$

where τ : shear stress (kPa)

τ_m: maximum shear stress (kPa)

k : Deformation contact of soil shear curve (mm)

Δ : shear deformation (mm).

Maximum shear stress τ_m is given as

$$\tau_m = C + \sigma \tan \phi \qquad (5.56)$$

where

C : Soil Cohesion (kPa)

σ : Normal Stress on Soil (kPa)

ϕ : Soil Internal Friction Angle

Figure 5.13 Shows the soil deformation under a rigid Wheel with slip s [4]. At any point x(mm) from the wheel leading edge, as a shown in the diagram, the shear deformation Δ is.

$$\Delta = sx$$

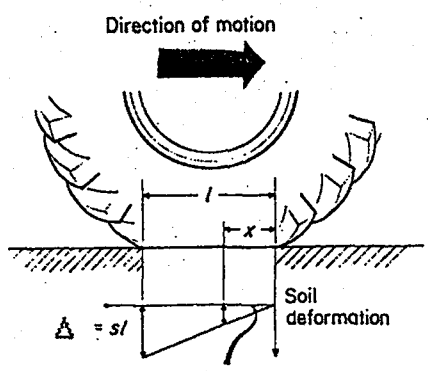

Figure 5.13. Soil Deformation under a Rigid Wheel With Slip S.

Equation (5.55) can therefore be written as

$$\tau = \tau_m (1 - \exp(- sx / k)) \qquad (5.58)$$

The thrust dT_{un} developed by an infinitesimal area dA can be written as follows.

$$dT_{un} = \tau . dA = \tau . b_i . d_x \qquad (5.59)$$

Assuming that the wheel operates at a constant wheel slip the total thrust developed by the unlugged area is given by the integration of equation (5.59) as follows

$$T_{un} = b \int_0^L \tau_m (1 - \exp(- \frac{sx}{K}) dx \qquad (5.60)$$

Solving the integration gives T_{un} as

$$T_{un} = \tau_m . b_i [L + k/s \exp(-SL/K)] + C_1 \qquad (5.61)$$

Using the boundary conditions, $T_{un} = 0$ when $L = 0$ the value of integration constant C1 in equation (5.61) is found as

$$C_1 = -\tau_m \, b_i \, k/s \qquad (5.62)$$

For an Iron-Wheel with soil contact area Aun, by using equations (5.56, 5.61 and 5.62) the thrust developed by lugged area is given by

$$T_{UN} = C. A_{UN} + Q \tan \phi [\, 1 - k/_{SL} + k/_{SC} \exp (-SL/_{k}) \,] \qquad (5.63)$$

where

$Q = \sigma_i \, . \, A_{UN}$: Loading acting on the rigid wheel.

If the sinkage is given as Z_{in} , then the length L of contact area would be found as follows.

$$L = 2 r_1 \sin (\cos^{-1} (1 - Z_{in} /r_1) \qquad (5.64)$$

The sinkage can be found by employing the an equation developed by Micklethwaite [8], which can be written as follows:

$$Z_{in} = Q^2 / (5.7 \, C)^2 \, b^2{}_i \, d_i. \qquad (5.65)$$

where

d_i = diameter of the Iron-Wheel

b_i = width of the Iron-Wheel

5.3.7 Rolling Resistance of an Iron-Wheel

Yong et al [38], while investigating track terrain interaction showed that the energy losses due to motion resistance were due to energy spent

(i) compacting the soil
(ii) shearing and distorting or disturbing the soil

Yong et al applied viscoplasticity technique to provide the basic energetics model for track terrain interaction. In this thesis a different model will be developed. This model is simpler, it can be readily used and it is expected to give fairly accurate value of rolling resistance. The contribution of rolling resitance due to compaction and shear and soil disturbance would be treated separately as the energy spent in compacting the soil is actually wasted energy while the other is not; this will be explained in detail later in the section

Rolling resistance due to compaction can either be dueto compaction of the soil by the unlugged area of the Iron-Wheel or the Iron-Wheel lugs. The compaction of the soil by Iron-Wheel lugscan be reduced to practially none through a proper choice of the lug inclination angle β . This aspect of Iron-Wheel design will be treated later.

Rolling resistance due to compaction by the unlugged area of the Iron-Wheel can be found by means of equation by Mikelethwaite

[8].

$$R_C = Q^2 / 5.7.\, c.\, b_i\, .\, d_i \qquad (5.66)$$

where

R_c : Rolling resistance due to soil compaction (kN).

c : Soil cohession (kPa).

b_i : iron-wheel width (m).

d_i : iron-wheel diameter (m).

Q : Load acting on the Iron-Wheel (kN)

The rolling resistance due to soil shearing and disturbance will be determined by calculating first the energy spent on shearing and disturbing the soil and then dividing it with the perimeter of Iron-Wheel. The energy spent by each lug is represented by the area under the curve of Figure 5.10. The total lateral displacement is given by the equation below

$$l_t = \frac{1}{2}\,[(r_1 \cos(\lambda_f - \phi_i) + r_2 \cos\lambda_f) - (\,(\lambda_L - \lambda_f)\, r_1 (1 - S) + r_1 \cos(\lambda_L - \phi_i) + r_2 \cos\lambda_L\,) \qquad (5.67)$$

$$Z_t = r_2 \sin \pi/2 - r_2 \sin\lambda_f - Z_{in} \qquad (5.68)$$

The energy spent by a lug is then given by

$$E_{SL} = \frac{0.7\, Z_t\, b_i\, L_H}{2} + b_i\, L_H \langle l_t - Z_t \rangle \qquad (5.69)$$

The second term of equation (5.69) is applicable only if the difference in the bracket is positive; in case the difference is negative

the lug lateral movement is smaller than the vertical depth and energy calculation only includes the triangular part of Figure 5.11.

If the total number of lugs on the Iron-Wheel is Ni, then the energy spent by Iron-Wheel per revolution is

$$E_{si} = N_i \cdot E_{SL} \tag{5.70}$$

The Iron-Wheel rolling resistance due to soil shearing and disturbance is

$$R_{LS} = \frac{N_i}{\pi d_i}\left[\frac{0.7\, Z_t\, b_i\, L_H}{2} + b_i\, L_H \langle l_t - Z_t \rangle\right] \tag{5.71}$$

The rolling resistance R_{LS} does not actually represent a parasitic force as is the case of R_C, but it is useful in the sense that it helps soil cultivation by shearing and disturbing a layer of soil Zt (mm) deep. Of course this will reduce the amount of energy spent in primary and secondary cultivation. Therefore the energy spent by the Iron-Wheel on shearing and disturbing the soil, E_{SI} would be lumped together with the energy used by the agricultural implement.

For the sake of quantifying the total rolling resistance experienced by an Iron-Wheel, the equation below will should be used

$$R_{tI} = Q^2 / 5.7\, c\, b_i\, d_i + \frac{N_i}{\pi d_i}\left[\left(\frac{0.7\, Z_t\, b_i\, L_H}{2}\right) + \langle b_i\, L_H [l_t - Z_t] \rangle\right] \tag{5.72}$$

where

Z_t : The lug's total depth.

l_t : The lug's total lateral disturbance.

L_H : The horizontal force required to cause soil failure given by equation (5.33)

5.3.8. Optimum Lug Inclination Angle

In specifiying the lug inclination angle β, the initial soil-lug interaction angle α_f should be carefully considered as the lug should pierce the soil instead of compressing it and thus increase rolling resistance. The initial soil-lug interaction angle α_f is given by the equation below

$$\alpha_f = \pi - \lambda_f - \beta \qquad (5.73)$$

The optimum lug inclination angle β_{opt} is such that $\alpha_f = \pi/2$. The value of β_{opt} is related to λ_f by the following equation

$$\beta_{opt} = \pi/2 - \lambda_f$$

As it was seen in the equations derived earlier, λ_f is not independent of β therefore β_{opt} could only be found after at couple of iterations. In this thesis the value of α_f will be allowed to vary between 1.40 and 1.75 radians.

5.3.9 Lug Spacing Criteria

As each of the Iron-Wheel lugs moves, it causes soil to fail and rupture a distance f. (refer to Figure 5.8), So as to avoid the lug from coming into contact with an already disturbed soil, the spacing between two consecutive lugs should at least be f mm; where f is the rupture distance as shown in Figure 5.8. From charts given in Ref [29] the value of f is given by the following relationship for each particular soil

$$f/_{Z_c} = m$$

where

f : rupture distance (mm)

Zc : lugs vertical depth (mm)

m : a constant depending on the angle α_f and soil internal friction, angle.

From the above equation, a relationship between the lug's vertical depth and the number of lugs on the Iron-Wheel N_i can be developed as

$$N_i = \frac{\pi d_i}{m Z_c} \qquad (5.76)$$

The number of lugs on an Iron-Wheel should be kept at minimum as the weight and cost of producing an Iron-Wheel undoubtly increases with increase in the number of lugs on the Iron-Wheel. The least number of lugs on an Iron-Wheel is the number of lugs in contact with soil at any moment that would allow

smooth transfer of power and a Jerk-free motion. This will be adopted as the minimum number of lugs on the Iron-Wheel. In this thesis the number of lugs in contact with soil at any moment will be taken as three as smaller numbers results in excessive lug forces and Jerky motion.

5.3.10 Iron-Wheel's Tractive Efficiency

It was seen in chapter two that tractive efficiency of the tractor driving wheels are among the most important parameters affecth the tractor's performance. It was therefore found of great importance to develop an equation for prediction the tractive efficiency of the Iron-Wheels and is given as

$$\eta_i = \frac{P_T\ (1-s)}{P_T + R_c}$$

where

PT : Summation of drawbar pull due Iron-Wheel lugs and the unlugged area of in Iron-Wheel contact with soil; given by the equation below

$$P_T = T_{un} + T_i$$

η_i : Iron-Wheel's tractive efficiency.

R_c : Rolling resistance due to compaction.

s : wheel slip.

CHAPTER VI

DETAIL DESIGN OF IRON-WHEEL FOR BAŞAK-17

6.1 Introduction

Among the greatest challenges that faces engineers is to design a product starting from a theoretical analysis and models; particularly in a field not attempted before. Such a challenge is faced here in designing an Iron-Wheel to be fitted Başak-17 tractor. By using equations derived in the previous Chapter. This challanges will be overcame here by designing the Iron-Wheel and predicting the performance of Başak-17 fitted with the Iron-Wheels.

After the functional and mechanical design have been done, the technical drawings required to have the Iron-Wheel manufactured will be given. To highlight the merits and shortcomings of using Iron-Wheels, the performance of Başak-17 fitted with Iron-Wheel will be compared to those obtained in Chapter four, for a Başak-17 tractor fitted with pneumatic tyres.

The design process of the Iron-Wheel will be explained after a short discussion on the importance of soil properties on the design of Iron-Wheel and this is done in the next section.

6.2 The Importance of Soil Properties on Iron-wheel Design

The property of the soil on which the tractor fitted with the Iron-Wheel will be used affects the specification of all the Iron-Wheel design parameters. This fact is clearly illustrated by observing that all equations derived to predict the performance of the Iron-Wheel in the previous chapter contains variables that represents at least one soil property. It is therefore important to realize that in order to have a well designed Iron-Wheel, detail data of the average soil conditions found in the intended area on which the Iron-Wheel would be used is required.

The soil properties assumed in the design of the Iron-Wheel for Başak-17 tractors be used in tropical arid and semi-arid regions of East the Central Africa is average soil condition found in East and Central Africa as represented by Crossley et al [10]. Table 6.1 shows the data for soil properties found in arid and semi-arid regions of East and Central Africa.

Table 6.1 Soil Properties Data [10].

Soil Property	Value
Soil Internal Friction Angle (in degrees)	10
Soil Density (kN/m^3)	2660
Soil cohesion (kPa)	40
Soil Adhesion (kPa)	85

6.3 Necessary Tractor Data for Iron-Wheel Design

Not only was it necessary to have soil property data for design of Iron-Wheel but tractor data is also necessary. Table 6.2 shows the necessary data that will be used to design the Iron-Wheel for Başak-17 for use in arid and semi-arid regions.

Table 6.2 Tractor Data Necessary for Iron-Wheel Design.

Parameter	Value
Engine torque (Nm)	: 49.1
Tractor Weight Acting or Rear Axle (n)	: 4900
Rear Tyre Diameter (mm)	: 814
Cultivation Speeds (ms^{-1})	: 0.88, 1.74

6.4 Iron-wheel's Functional and Mechanical Requirements

The Iron-Wheel's design cannot be undertaken without first setting up the minimum performance requirements to be satisfied during the design process. These performance requirements are divided into functional and mechanical requirements. The functional requirement is defined as the required ability of the Iron-Wheel to perform the functions it was designed for, which are

(i) It's ability to enhance the tractor's drawbar pull. That is in other words, when Başak-17 is fitted with iron-wheels the tractor's drawbar pull should be above 5000N so as to

enable the tractor to be utilized successfully in tropical arid and semi-arid regions.

(ii) It's ability to improve the tractor's tractive efficiency when used in tropical regions.

(iii) It's ability to provide a smooth motion for the tractor.

The mechanical requirement of the Iron-Wheel is defined as the requirements that should be taken into account and fulfilled during the mechanical design stage. The mechanical requirements include

(i) The ability of the Iron-Wheel to withstand the forces experienced during primary cultivation which include the drawbar pull, tractor weight acting on the rear axle and axle torque.

(ii) The Iron-Wheel lug's should have wear resistance as the dry soil is abrasive and causes rapid wear of metallic parts.

(iii) The Iron-Wheel should be easy to fix to the tractor axle and portable by a single person.

(iv) It should have a design life of minimum 8 years.

(v) It should be easy to manufacture and should contain minimum parts

(vi) It should be easy to repair and maintain.

All the requirements mentioned above will be satisfied during the Iron-Wheel functional and mechanical design done in the following sections.

6.5 Iron-Wheel's Functional Design

6.5.1 Parameters Affecting Iron-Wheels Functional Performance

Functional design of the Iron-Wheel is termed as the specification of the Iron-Wheel design parameters affecting it's functional performance. These design parameters will be grouped for discussion and specifications under the following headings

(i) Iron-Wheel 's diameter, d_i and width b_i.

(ii) Lug inclination angle β.

(iii) Lug's depth, Z_i and Number of lugs on the Iron-Wheel, N_i.

6.5.1.1 Specification of Iron-wheel's Diameter, d_i and Width b_i

Not much option is there in the specification of Iron-Wheel's diameter but to make it approximately equal to the Başak-17 tractor's rear tyre's diameter, which is about 814 mm.

For the specification of the Iron-Wheel width, it is important that the Iron-Wheel's width be made large when compared to the lug's depth in the soil, so as to have an approximately two dimensional soil failure at the lug-soil interface. Apart from the constraint mentioned above, the width of the Iron-Wheel can be varied until the required drawbar pull from the Iron-Wheel is obtained.

The width of the Iron-Wheel designed for Başak-17 to be used in arid and semi-arid regions will be initially, taken as 300 mm and will be increased if necessary to obtain the required drawbar pull

for primary cultivation; which is about 5000N.

6.5.1.2 Specification of Lug Inclination Angle, β.

It was stated in the previous Chapter that improper choice of lug soil compaction inclination angle β results in the increase of both the Iron-Wheel's rolling resistance, the stresses in lugs cross section area and soil compaction by lugs. It was therefore stated that the lug inclination angle should be chosen such that the initial soil-lug interaction angle α_f will have a value between 1.40 and 1.75 radians;

The lug inclination angle β is chosen as $\pi/6$ and it will be shown that the initial soil-lug interaction angle α_f will have a value between 1.40 and 1.75 radians.

6.5.1.3 Lug's Depth Z_i and the Number of Lugs on the Iron-Wheel, N_i.

Optimum lug spacing criterion was developed in the previous chapter and a relationship between the lug's depth and the number of lugs on the Iron-Wheel was developed and given by equation (5.76)

$$Z_i = \frac{\pi d_i}{mN_i}$$

where m in equation (5.32) is a variable whose value depends on the soil internal friction angle and soil -lug interaction angle, refer to Ref [29].

The lug's depth is inversely proportional to the total number of lugs on the Iron-Wheel. That is if the lug depth is increased the number of lugs on an Iron-Wheel decreases and vice versa, provided the soil internal friction angle and soil-lug interaction angle are kept constant.

To specify the values of the lug's depth and the number of lugs on the Iron-Wheel, the minimum number of lugs in contact with the soil criterion will be used. This criterion can be stated as follows, the minimum number of lugs in contact with soil at any time should be such that a smooth transfer of power and a Jerk free motion results. This number was taken as three in the previous Chapter.

The average number of lug in contact with soil at any time is given by equation (6.1)

$$N_L = \frac{\phi_L N_i}{\pi} \qquad (6.1)$$

where the angle ϕ_L is given by equation (6.2) below

$$\phi_L = \lambda_L - \lambda_f \qquad (6.2)$$

where

N_L : Average number of lugs in contact with the soil

λ_L : Lug's last contact angle

λ_f : Lug's first contact angle

N : Total number of lugs on the Iron-Wheel

The minimum number of lug's in contact with the soil criterion can be mathematical stated by using equation (6.1) as

$$\frac{\phi_i N_i}{\pi} > 3 \qquad (6.3)$$

For Iron-Wheels of Başak-17 tractor's rear tyres sizes it was found that the angle ϕ_L can be taken as about 0.436 radians. The minimum number of lugs on the Iron-Wheel is then given as

$$N_i > 21.6 \qquad (6.4)$$

For the sake of having a symmetrical Iron-Wheel the value of Ni is given by equation (6.5) below

$$N_i = 24 \qquad (6.5)$$

The specification of the lug's depth would be done by using equation (6.1) and by taking m = 2.4, this is done because the soil-lug interaction angle is changing and thus m would vary between approximately 1.8 to 2.6. The lug's depth is then given by equation (6.6) below

$$Z_i = \frac{\pi \times 814}{2.4 \times 24} = 44.4 \text{ mm}. \qquad (6.6)$$

After having specified the design parameters affecting the functional performance of the Iron-Wheel, the remaining important parameter necessary for prediction of the performance of the Iron-Wheel would be calculated in the next section.

6.5.2 Calculation of the Remaining Important Parameters

The detailed description of the parameters to be calculated in this subsection is given in the previous chapter and the reader is requested to refer to the previous chapter if the description in this subsection is not enough.

(i) Iron-Wheel sinkage.

The Iron-Wheel sinkage could be calculated by using equation (5.65) as shown below

$$Z_{in} = Q^2 / (5.7\ c)^2\ b_i^2\ d_i \quad mm \tag{5.65}$$

where

Q : Load acting on the Iron-Wheel (kN)

c : Soil cohesion (kN/mm).

b_i : Iron-Wheel width (mm).

d_i : Iron-Wheel diameter (mm).

Z_{in} : Iron-Wheel sinkage (mm).

The sinkage is found as

$$Z_{in} = 1.52 \text{ mm} \tag{6.7}$$

(ii) Lug's length, Z.

The lug's length could be calculated by using equation (5.54) as shown below

$$Z = Z_i / \cos\beta \quad (mm) \tag{5.37}$$

and the lug's length is taken as

$$Z = 52 \ mm \tag{6.8}$$

where

Z_i : Lug's depth

β : Lug inclination angle.

(iii) Calculation of parameters necessary for the lug displacement

equations are done below

$$\phi_i = \tan^{-1}\left[\frac{\text{Sin}\,\beta}{r_1 / Z + \text{Cos}\,\beta}\right] \ (\text{radians}) \tag{5.36}$$

$$\phi_i = 0.0574 \text{ radians} \tag{6.9}$$

$$r_2 = \frac{Z \,\text{Sin}\,\beta}{\text{Sin}\,\phi_i} \quad (mm) \tag{5.37}$$

$$r_2 = 452.00 \ \ mm \tag{6.10}$$

$$\phi_L = \text{Cos}^{-1}\left[\frac{r_1 - Z_{in}}{r_2}\right] \text{ (radians)} \qquad (5.39)$$

$$\phi_L = 0.4576 \text{ radians} \qquad (6.11)$$

$$\lambda_f = \pi/2 - \phi_L \text{ (radians)} \qquad (5.38)$$

$$\lambda_f = 1.113 \text{ radians} \qquad (6.12)$$

$$\lambda_f = \pi/2 + \phi_L \text{ (radians)} \qquad (5.38)$$

$$\lambda_f = 2.0283 \text{ radians} \qquad (6.13)$$

iv) Avarage number of lugs in contact with the soil, N_L.

N_L could be calculated by using equation (6.1) as shown below and fixing the values of ϕ_L and N_i.

$$N_L = \frac{\phi_L N_i}{\pi} \qquad (6.1)$$

$$N_L = 3.496$$

Thus the minimum number of lugs in contact with the soil criterion is satisfied as the avarage of lugs in contact with the soil is more than three at any time.

v) Lug inclination angle β.

When specifying lug inclination angle β it was said that this angle should be specified such that the initial lug-soil interaction angle α_f has a value between 1.40 and 1.75 radians. Now since all the design parameter have been calculated the initial lug-soil interaction angle α_f is found by using equation (5.) as shown below

$$\alpha_f = \pi - \lambda_f - \beta \quad \text{(radians)} \tag{5.73}$$

$$\alpha_f = 1.5048 \quad \text{radians} \tag{6.13}$$

Thus lug inclination angle β was properly chosen and satisfies the condition that the initial lug-soil interaction angle be between 1.40 and 1.75 radians.

A summary of the specified and calculated parameters are given in Table 6.3 in a summarized form.

Table 6.2 Iron-wheel Parameters

Parameter	Value
Z (mm)	52
Z_i (mm)	45
Z_{in} (mm)	1.52
r_i (mm)	407
r_2 (mm)	452
b_i (mm)	300
N_i	24
N_L	3.496
ϕ_i (radian)	0.0574
ϕ_L (radian)	0.4576
λ_L (radian)	2.0283
λ_f (radian)	1.1130
α_f (radian)	1.5048
β (radian)	0.5236

6.6 The predicted performance of Başak-17 fitted with the Iron-Wheel.

6.6.1 Introduction

After having completed the Iron-Wheel's functional design it is only natural to check whether the Iron-Wheel 's performance satisfies the functional requirement stated earlier in the chapter. If the Iron-Wheel's functional performance does not satisfy the functional requirements, the functional design has to be repeated. The Iron-Wheel functional requirements include its ability to enhance the tractor's drawbar pull and tractive efficiency and therefore both the tractor's drawbar pull and tractive efficiency when fitted with the Iron-Wheel designed earlier will be predicted in the next subsections.

6.6.2. Prediction of Tractor's Drawbar Pull.

6.6.2.1 Drawbar Pull Contribution From Iron-Wheel Lugs

When an Iron-Wheel is fitted to a tractor both the Iron-Wheels lugs and the Iron-Wheels unlugged area in contact with the soil contribute to the tractor's drawbar pull. In this subsection only the contribution by Iron-Wheel lugs in contact with the soil will be predicted by using equations derived in the previous Chapter and are given below as

$$T_i = \sum_{i=1}^{N_Z} b_i [P_i L_i \sin(\lambda_i + \beta - \delta) - Ca Z_i \cos^2(\lambda_i + \beta)] \qquad (5.52)$$

where

$$L_i = Y\ Z_i^2\ N_{\mu i} + C_c\ N_{ci}\ Z_i + Ca\ N_{ai}\ Z_i + q_i\ Nq_i\ Z_i \qquad (5.54)$$

and

$$Z_i = r_2 \sin \lambda_i - r_2 \sin \lambda_f - Z_{in} \qquad (5.45)$$

As it could be observed from the equations above the drawbar pull from each lug is a function of the lug λ_i and the angle λ_i for any lug i is related to the leading lug angle λ_1 by equation (6.15) below

$$\lambda_i = \lambda_1 + \epsilon\,(i-1) \qquad (6.15)$$

where

$$\epsilon = \frac{2\pi}{N_i} \qquad (6.16)$$

and i is the position of the lug from the leading lug as shown in Figure 6.1 given below

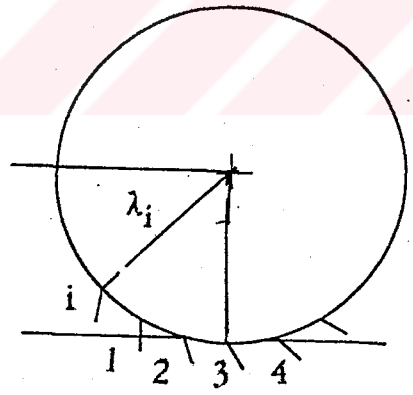

Figure 6.1. Schematic Diagram of the Iron-Wheel.

The drawbar pull obtained from Iron-Wheel lugs is then a function of the leading lug angle λ_1. To obtain a representative value for the drawbar pull, two leading lug angles will be chosen at which the drawbar pull will be predicted and these angles are given as

$$\lambda_1 = \lambda_f \tag{6.17}$$

$$\lambda_1 = \lambda_f + \epsilon/2 \tag{6.18}$$

when $\lambda_1 = \lambda_f$, the instantaneous drawbar pull of the Iron-Wheel shown in Figure 6.1 is given and when $\lambda_1 = \lambda_f + \epsilon/2$ the instantaneous drawbar pull of the Iron-Wheel after the Iron-Wheel has rotated through an angle $\epsilon/2$ is given. The instantaneous drawbar pull after the Iron-Wheel has rotated through an angle ϵ is equivalent to that obtained when $\lambda_1 = \lambda_f$ because the Iron-Wheel lugs arrangement at $\lambda_1 = \lambda_f$ and $\lambda_1 = \lambda_f + \epsilon$ are equivalent to each other. The two angles chosen at which the drawbar pull are calculated are thus representative enough.

The details of the methodology for calculating the drawbar pull contribution from Iron-Wheel lugs is given in A.1, the summary of the results is tabulated in Table 6.4 below.

Table 6.4 Drawbar Pull from Iron-Wheel Lugs.

Leading angle, λ_1 (radians)	T_i (kN)
$\lambda_1 = \lambda_f = 1.07$	4.18
$\lambda_1 = \lambda_1 + \epsilon/2 = 1.33$	3.45
Avarage drawbar pull at $\lambda_1 = \lambda_f$ and $\lambda_1 = \lambda_f + \epsilon/2$	3.82

6.6.2.2. Drawbar Pull Contribution from Iron-Wheel's Unlugged Area.

The drawbar pull contribution from the unlugged area of the Iron-Wheel can be calculated by means of equation (5.63) written below. This equation was derived in the previous chapter.

$$T_{un} = C.A_{un} + Q \tan [1 - K/_{sL} + K/_{sL} \exp (sL/_{K})] \qquad (5.63)$$

Table 6.5 gives the values for the various parameters given in equation (5.47). These values are for soil parameters, tractor parameter and Iron-Wheel parameter which are taken from Tables (6.1, 6.2 and 6.3) and calculated by using data given in the aforementioned tables and equations derived in the previous chapter.

Table 6.5 Values for Various Parameter is of Equation (5.47)

Parameter	Value
Assumed Wheel Slip, S.	0.15
Soil Cohesion (kN/m^2), C.	40
Soil Internal Friction Angle(radians), ϕ.	0.175
Tractor Weight Acting on the Iron-Wheel (kN), Q.	2.40
Iron-Wheel Contact Length (m), k.L	0.07
Soil Deformation modulus (m), K	0.04
Wheel-Soil Contact Area (m^2), A_{un}	0.021

By using equation (5.47) and values given in Table (6.5), the drawbar pull contribution the Iron-Wheel's unlugged area is given by equation (6.19)

$$T_{un} = 1.131 \text{ KN} \tag{6.19}$$

The Tractors total drawbar pull, P_T, when fitted with the Iron-Wheel was calculated as

$$P_T = 2 (T_i + T_{un}) = 9.90 \text{ KN} \tag{6.20}$$

and this value is much higher than the value set for the functional requirement in section 6.2 which is 500o N. Thus the functional design has design has been successful in fulfilling the drawbar pull requirements. The other Iron-Wheels functional requirement that would be checked it is fulfilled is if the the Iron-Wheel enhances the tractors tractive efficiency but before this is done the Iron-Wheels rolling resistance need to be predicted and this is done below.

6.6.3 Prediction of Iron-Wheel's Rolling Resistance

It was stated is the previous chapter that the Iron-Wheel's rolling resistance is divided into two parts and these are the rolling resistance due to Iron-Wheel soil is compaction by is given equations (5.66) and that due to soil shearing and distortion is given by equation (5.67). which are both written below

$$R_c = Q^2/5.7\, c\, b_i\, d_i \qquad (5.66)$$

$$R_s = \frac{N_i}{\pi d_i}\left[\frac{(0.7\, Z_t\, b_i\, L_H)}{2} + \left\langle b_i L_H\,(L_t - 0.7\, Z_t)\right\rangle\right] \qquad (5.67)$$

The total rolling resistance experienced by the Iron-Wheel is simply the addition of the rolling resistance due to soil compaction and that due soil shearing and distortion. Table 6.6 gives the values of the parameter necessary to calculate the Iron-Wheels rolling resistance By using the values for the various parameter given. In Table 6.6. and equation.

Table 6.6 Necessary Data for Calculating the Rolling Resistances

Parameter	Value
Soil Cohesion (KN/m^2), C.	40
Load Acting on Iron-Wheel (kN), Q	2.40
Iron-Wheel Diameter (m), d_i	0.814
Iron-Wheel Width (m), b_i	0.300
Number of Lugs on Iron-Wheel, N_i	24
Horizontal Force Acting on Soil-Lug Interface (kN/m) for $Z_i = Z_t$, L_H	8.296
Max. Depth of Lug in Soil (m), Z_t	0.045
Max. Lateral Displacement of Lug (m), L_t	0.044

in Table 6.6. and equations (5.51) and (5.52) the rolling resistances are calculated and tabulated in Table 6.7 below.

Table 6.7 Iron-Wheel Rolling Resistances

Rolling Resistance	Value
Due to Soil Compaction (N), R_c	103.4
Due to Soil Shearing and Distribution (N), R_s	664.4
Total Rolling Resistance (N), R_T	767.8

6.6.4 Prediction of Tractor's Tractive Efficiency

As the predictions of the tractor's drawbar pull and rolling resistance experienced by Iron-Wheel have already been done, the tractor's tractive efficiency will now be easily predicted by using equation (5.57) derived in the previous chapter. This equation is rewritten below as

$$\eta_i = \frac{P_N(1 - s)}{P_N + R_C + R_f}$$

Equation (5.57) will be used to predict the tractive efficiency of Başak-17 when fitted with Iron-Wheels. Tables 6.8 gives the values of the various parameters required to calculate the tractor's tractive efficiency. The tractor's tractive efficiency is given by

Table 6.8 Necessary Data for Calculating the Tractive Efficiency.

Parameter	Value
Net drawbar pull from the tractor (N), P_N	9.56
$P_N = 2 (T_i + T_{un} - R_c - R_f)$	
wheel slip, s	0.15
Iron-Wheel's rolling resistance due to compresion (kN), R_c	0.103
Tractor's front Wheel Rolling Resistance (N), R_f (see A.2)	0.072

equation (6.19)

$$\eta_i = 82\ \% \qquad (6.21)$$

Equation(6.19) shows that the tractor's tractive efficiency is higher than that obtained when the tractor is fitted with pneumatic tyre (refer to chapter IV). Since both the tractor's drawbar pull and tractive efficiency are enhanced when it is fitted with Iron-Wheels, the Iron-Wheels functional design can be said to be successful.

6.7 Mechanical Design of the Iron-Wheel.

6.7.1 Introduction

The Iron-Wheel's mechanical design will be done while keeping the Iron-Wheel's mechanical requirements discussed earlier in the chapter in mind. To fulfill the Iron-Wheels mechanical requirements

the Iron-Wheels mechanical design will be done under the following headings,

i) Design for strength and durability.

ii) Design for easy handling, maintanance and repair.

iii) Design for easy manufacture.

6.7.2 Design for Strength and Durability

The forces experienced by the Iron-Wheel are in most part alternating and therefore the Iron-Wheel will have to be designed for fatigue strength. The Iron-Wheel's design life for fatique strength will be taken as 8 years. The number of cycle experienced by the Iron-Wheel during it's life is given by the equation below

$$C_n = \frac{3600\, Y_s \cdot H_y \cdot V_h}{\pi d_i}\ 21.17 \times 10^6 \text{ cycles.} \qquad (6.22)$$

where

C_n : The number of cycles experienced by the Iron-Wheel.

H_Y : Assumed tractors utilization hours per year (1000 hrs).

V_h : The tractor's top cultivation speed in ms^{-1} (1.88 ms^{-1}).

d_i : Iron-Wheel's diameter in m (0.814 m)

Y_s : Iron-Wheel's design life in Years (8 Years)

3600 : Conversion factor from hour to Second.

The material specified for the manufacture of Iron-Wheel part experiencing alternating forces should be chosen to have a life of above 21.17 x 10^6 cycles for the load experienced.

During operation Iron-Wheel lugs will be operating under very harsh condition and to ensure it's durability, the material from which they'll be manufactured should have the following characteristics.

(i) It should be able to withstand the wear due to the abrasive soil particles

(ii) It should be tough and able to withstand shock loads.

(iii) It should have high fatique strength.

The materials given in Table 6.9 satisfy the requirements given above for the specification of material to be used to manufacture the Iron-Wheel lugs. Of course there are other, material not included in the table that could have been used for the manufacture of the Iron-Wheel lug but the final choice of the material should be done after field experiments and cost analysis.

Table 6.9 Some Possible Lug Materials [42, 43].

Material		Composition										
		C	Mn	P	S	S	Cr	Va	W		Mo	Ni
Chrome-Vanadium Steel-1	L H	0.45 0.55	0.50 0.80	- 0.040	- 0.040	- -	0.80 1.10	0.15 0.2	- -	- -	- -	
Chrome Vanadium steel-2	L H	0.65 0.75	0.10 0.30	- 0.030	- 0.030	0.25 0.35	0.70 0.90	0.15 0.25	- -	- -	- -	
Chrome-Vanadium Steel-3 (300-m)	L H	0.26 0.31	0.65 0.95	- 0.035	- 0.035	1.45 1.80	0.65 0.90	0.05 0.15	- -	0.,36 0.45	1.65 2.00	
Low-Tungsten Steel	L H	0.40 0.50	0.15 0.35	- 0.025	- 0.025	0.15 0.35	1.25 1.50	0.15 0.25	2.00 3.00	- -	- -	

6.7.3 Design for Easy Handling, Maintanance and Repair.

Since the Iron-Wheel is all metallic, it will be rather heavy. The weight of the Iron-Wheel should be kept at levels that one person can quite easily lift and fit it. A light and portable Iron-Wheel will be cheaper and would require less time and no special jigs during fitting unlike a heavier one.

Design calculations (see Appendix : 3) show that an all steel Iron-Wheel will weigh about 90 kg, Such an Iron-Wheel is not portable at all and therefore a lighter material should be specified for Iron-Wheel parts not experiencing high stresses and shock loads. This approach means that the Iron-Wheel will consist of two general parts, parts manufactured from alloy steel which experiences high stresses and shock loads, which include the lugs and a rim. Manufactured from a light material, which does

Table 6.10 Some Aluminium Alloy [44].

Alloy number* and Temper†	Fatigue Strength St (MPa)≠
LM5-M	95
LM10-TB	55
LM18-M	55
LM2-M	55
LM12-TF	60
LM16-TB	70
LM25-TF	60

* British BS 1490 designation.
† M, as manufactured; TB, solution treated; TF solution treated and precipitation treated.
≠ Fatique strength for $50x\ 10^7$ cycles.

not experience high stresses and shock loads. Any of the aluminium alloys given in Table 6.10 can be specified for the manufactured of the Iron-Wheel rim.

To ease maintainance and repair, the lugs should be designed to be assembled to Iron-Wheel rim. In that if one or more lugs break during service, the Iron-Wheel lugs could be replaced instead of scrapping the whole wheel.

The cheapest separable connections between the Iron-Wheel rim and lugs is achieved by using threaded fasterners. To reduce the number of fasterners and time required for the Iron-Wheel assembly, Iron-Wheel shoes will be used. An Iron-Wheel shoes is an all cast part consisting of three lugs on an arc platform which have threaded holes for fastening the shoes to the Iron-Wheel rim. The technical drawing of the Iron-Wheel shoe is appended to this thesis.

The use of an almunium alloy rim reduces the weight of the Iron-Wheel to about 55 kg, which is a portable weight and such an Iron-Wheel is easy to handle.

6.7.4 Design for Easy Manufacture.

Sand casting is chosen as the method for manufacturing the Iron-Wheel as it is highly productive and inexpensive [45]. In the design of the Iron-Wheel rim and shoes every effort will be made to reduce the number of cores required in the molds.

The design is also made for easy machining of the necessary Iron-Wheel surfaces and bores by allowing for tool overtravel and easy asses of machine tools to the surfaces to be machined.

The Iron-Wheel assembly is made easy by using Iron-Wheel shoes, instead of connecting every lug to the Iron-Wheel rim by using fasteners or welding and by reducing the welded surfaces to only two.

6.8. Comparative Performance of Başak-17 When Fitted with Iron-Wheel and Pneumatic Tyres.

Among the main reason for designing the Iron-Wheel was to improve the operational performance of Başak-17 tractor for arid and semi-arid region, which was very poor for Başak-17 fitted with pneumatic tyres. (see Chapter four). It was therefore of interest to check whether this enhancement of performance was actually achieved by comparing the performance of Başak-17 when with Iron-Wheel and pneumatic tyres The performance of Başak-17 filled with pneumatic tyres will be predicted by using equations (2.5, 2.8-2.19), introduced in chapter II. The detailed methodology for

predicting the functional performance is given in the Appendix. Here only the result will be given as tabulated in the second column of Table 6.11.

Most of the functional performance parameters for Başak-17 fitted with Iron-Wheel has already been predicted in the previous subsections but the parameters that include work-rate and percentage engine power utilization need to be predicted. The percentage engine power utilization will be predicted by using equation (6.23)

$$P_u = \frac{P_N V}{\eta_t P_e} \times 100 \qquad (6.23)$$

where

P_N : Net tractor drawbar pull, N (kN = 9560 N)

V : Tractor's cultivation speed, ms^{-1} (V = 0.748).

η_t : The tractor's transmission efficiency (η_t = 0.9).

P_e : Tractor's nominal engine power, kW (P_e = 12.68)

P_u : Percentage engine power utilization (P_u = 62.7 %)

In calculating the tractor work-rate the assumption that the tractor's work-rate is directly proportional to the tractor's drawbar pull will be made. Actually this is a true if the soil condition and cultivation speed are constant. Since the work-rate of Başak-17 when fitted with pneumatic tyres is already known from chapter four the work-rate of Başak-17 fitted with the Iron-Wheel will be determined using this method. The ratio of the drawbar pull of the

tractor fitted with Iron-Wheel to that of the tractor having only pneumatic tyres will be found and this will be multiplied to the work-rate of the tractor having pneumatic tyres, thus the work-rate of the tractor with Iron-Wheels is obtained. The functional performances of Başak-17 with Iron-Wheel is Table 6.11.

Table 6.11 Comparison of the Performance of Başak-17 When Fitted with Iron-Wheels and Pneumatic Tyres

Tractor Parameter*	Tractor fitted with Pneumatic tyres	Tractor fitted with the iron-wheel
Net tractor drawbar Pull. (N)	2414	9560
Tractive efficiency (%)	72.0	82.0
Percentage engine Power utilization	15.8	62.7
Work-rate (ha/day)	0.51	2.02

* All tractor parameters were calculated in the following conditions.
wheel slip = 0.15
Soil cone index value = 1500 kPa
Soil conditions given in Table 6.1.

It can be observed from Table 6.11 that the Iron-Wheel improves the performance of Başak-17 tractor by almost 4 times. In other words the performance of Başak-17 fitted with the Iron-Wheel is better than the performance of four Başak-17 tractors connected in row. Considering this performance enhancement, it will be a waste of time, money and energy not to use Iron-Wheels for all small tractors the size of Başak-17.

CHAPTER VII

CONCLUSION

It was pointed out at the beginning of this thesis that in order to increase the agricultural production in developing countries and especially in Kenya, the agricultural activity need to be mechanized. As most of the farming in Kenya is done on relatively small sized farms (see sec.1.1), a small tractor with engine power output of less than 15 Kw was found to be a feasible mechanization tool from the point of view of farm power requirement and estimated production cost.

After having more or less picked up the tractor's engine power output, the engineering challenge was to ensure that the operational performance of the small tractor is as good as those of medium and large tractors. On this line the first step taken was to get a better understanding of how various parameters affect a tractor's operational performance. An in depth analysis was done on the critical parameters affecting a tractor's performance. This brought to light how the various tractor and soil parameters affect the tractor's operational performance. Equations to predict the tractor's operational and general performance were given.

The above mentioned equations were used to check the

suitability of three models of small tractors for cultivation of arid and semi-arid regions. Two models namely single-axle tractors and winch-type tractors were found to be unsuitable due to their poor operational and general performances. Though the third model namely a small 4-wheel ride-on tractor, represented by Başak-17 tractor also had poor operational performance in terms of low drawbar pull and tractive efficiency, it was found most promising in that it had a higher general performance and it is a feasible mechanization tool if it's operational performance could be improved.

To improve the operational performance of Başak-17 the use of Iron-wheels was proposed. In order to predict to operational performance of Başak-17 when fitted with Iron-wheels, the Iron-Wheel's lug-soil interactions were modelled by the use of passive earth pressure theory and the model was made to take into account the soil's compressibility. Equations to predict tractors drawbar pull, tractive efficiency and rolling resistance were derived and a rational design procedure for designing an Iron-Wheel was developed.

Functional and mechanical design of Iron-Wheel for Başak-17 was done and various important design considerations including reduction of Iron-Wheel weight and increasing the Iron-Wheel durability were done. Equations mentioned above were used to predict the operational performance of the tractor when fitted with the Iron-Wheel. The theoretically predicted results show that the drawbar pull of Başak-17 is improved by about 300%, which is well above that required for cultivation of arid and semi-arid region.

It is worth mentioning that the research work given in this thesis is unique in that no other researcher have attempted to solve the poor operational performance of a small 4-wheel ride-on when used in arid and semi-arid region by using and Iron-Wheel. It is important also to note that apart from equation (5.31) given by Reece [29] all the equations for modelling the soil-lug interactions are derived in this thesis.

This research is not only relevant to tropical countries with large percentage of their agricultural land consisting of arid and semi-arid regions but to any country with a considerable number of small farms. Of course Türkiye is included in the countries with a considerable number of small farms, as farms with sizes between 0.1-10 hectares makes 86% of the total farms as reported by Harzadın [46]. The number of tractors used in small farms in with sizes 0.1-10 ha is only 3% of the total tractors in use in the agricultural sector [46]. Therefore the mechanization of small farms in Türkiye is far from over and Başak-17 tractor fitted with Iron-Wheels could play an important role in the mechanization program.

The following are the useful extensions of this work, which are in scope complementary to this thesis.

a) The possibility of using other lug shapes and lug pattern can be investigated with optimization in mind. However, the optimal lug shape and pattern should conform to the primary design requirements.

b) It was stated in the thesis that Başak-17 tractor's overall design performance need to be evaluated. It is believed that very useful improvement are possible which will enhance the marketing chances of Başak.

REFERENCE

[1] Adema, W. "General Report on the Future Role of the Agricultural Machinery Industry in Developing Countries". Second International Conference on Development of the Agricultural Machinery Industry in Developing Countries .(1984.)

[2] Munga, S.N. "The Position of Farm Machinery Development in Kenya" Second International Conference on Development of the Agricultural Machinery Industry in Developing Countries .(1984.)

[3] Mrema, G.C. "Agricultural Mechanization in Tanzania-Constraints and Prospects" Second International Conference on Development of the Agricultural Machinery Industry in Developing Countries . (1984.)

[4] Crossley, C.P. Small Farm Mechanization for Developing Countries. (1983.)

[5] Grecenko, A "Predicting the Performance of Wheel Tractors in Combination with Implement" J. Agric Engng. Res. 13 (1)(1968.)

[6] Salegue U.M.and Jangier, A.A. "Optimization of the Operational parameters of a Wheeled Tractor for Tillage Operations". American Society of Agricultural Engineers. 33 (4). (1990.)

[7] Gee-clough, D. " Selection of Tyres Sizes for Agricultural Vehicle" J. Agric Engng Res. 25. (1980)

[8] Placket, C.W. 1985. "A Review of force prediction Methods for off-roadwheels" J. Agric Engng Res. 31 (1). (1985.)

[9] Gee-Clough, D., Mac Allister, M. Pearson, G. and Evernden, D.W. "Empirical prediction of tractor-implement field performance" Journal Terramechanics. 15 (2)(1978.)

[10] Crossley, C. P. and Kilgour, J. " The Development and Testing of a Winch- based small Tractor for Developing Countries" J. Agric Engng Res. 27.(1983.)

[11] Lara-lopez, A., Chancellor, W.J., Kepner, R.A. and Kaminaka, M.S. "A Two Wheeled Tractor for Manufacture in Mexico" Transaction of the ASAE. 25.(1982.)

[12] Kyeong U.K. and Reh Kugler, G.E. " A Review of Tractor Dynamics and Stability" Transaction of the ASAE. 30.(1987.)

[13] Crossley, C.P."Rural Transport in Developing Countries-The Development of the 'Carta' Computer Program" J. Agric Engng Res. 27(1982)

[14] Gee-Clough, D. and Sommers, M.S. "Steering Forces on Undriven, Angled Wheels" J. Terramechanics 18 (1)(1981).

[15] Gayı, D.A. "Design Criteria of Farm Machinery from Management Point of View": Second International Conference on Development of the Agricultural Machinery Industry in Developing Countries . (1984)

[16] Esmay, K. L. "Local manufacturing for small farms in East Asia" Transaction of the ASAE . 22.(1979.)

[17] Wal, Ullah, Md. Kofced, S.S. and Pederson, T.T. "Comparative performance of four-wheel tractor and two-wheel tractor in small plots" Agricultural Mechanization in Asia, Africa and Latin America. 20 (1)(1989.)

[18] _____ , "Another New One for Kenya". Nation Daily News. (16 September 1991).

[19] Ancheta, C.J. and Bautista, R.C. "Work Capacities and fuel consumptions of Hand tractor manufactured in the Philippines" Agricultural Mechanization in Asia, Africa and Latin America. 17 (2)(1986.)

[20] Doğan Erdoğan. "A study on Field Performance of Small Tractors" Agricultural Mechanization in Asia, Africa and Latin America. 18 (3)(1987).

[21] Crossley, C. P. and Kilgour, J. "Field Performance of a Winch-powered Cultivation Devices in Central Africa" J. Agric Engng Res. 23.(1978).

[22] Crossley, C. P. and Kilgour, J. 1983. "The Development and Testing of a Winch-Based Small Tractor for Developing Countries" J. Agric Engng Res. 28.(1983).

[23] _____, Driver's Handbook. Türkiye Zirai Donatım Kurumu Genel Müdürlüğü.

[24] _____ , Advertizing Brochures. Türkiye Zirai Donatım Kurumu Genel Müdürlüğü.

[25] Sakai, Jun Phongsupasamit, S. and Kıshimoto. "A Study on Engineering Design Theories of an Iron-Wheel for Plowing". AMA. 18 (4)(1987).

[26] Takashi Tanaka. "Operation in Pucdy Fields : State of the art report" Journal of Terramechanics 21 (2)(1984).

[27] Hettiaratchi D.R.P., and Reece, A.R. "The Calculation of Passive Soil Resistance" Geotechnique. 24 (3)(1974.).

[28] Jo Yung Wong "Book Review : Soil Mechanics for off-road Vehicle Engineering" Journal of Terramechanics. 16 (4)(1979).

[29] Hettiaratchi, D.R.P., Witney, B.D. and Reece, A.R. "The Calculation of Passive Pressure in Two-Dimensional Soil Failure" J. Agric Engn. Res . 11 (2)(1966).

[30] Tomio Ito and Mamoru Aoyama. "Thrust and Slip Line Analysis of One Track Shoe". Journal of Terramechanics . 19(3)(1982).

[31] Salokhe, V.M., Manzoor, S. and Gee-Clough, D. "Pull and Lift Forces Acting on Single Cage Wheel Lugs". Journal of Terramechanics. 27 (1)(1990).

[32] Gee-Glough, D. 1976 "Pull and Lift Characteristics of Single Lug Rigid WHeels in Wet Rice Soil Frams" Transaction of the ASAE. 19 (3)(1976).

[33] Beker, M.G. Introduction to Terrain-Vehicles System. The University of Michigan Press . Ann Arbor.(1988).

[34] Stafford, J.V. "The Performance of a Rigid Line in Relation to Soil Properties and Speed" J. Agric Engn Res. 24 (1)(1979).

[35] Nowatzki, E.A. and Karafiath, L.L. "General Field Condition in Plasticity Analysis of Soil Wheel Interaction". : Journal of Terramechanics . 11 (1)(1974)

[36] Terzaghi, K. : Soil Mechanics in Engineering Practice . John Willey & Sons Inc.(1960)

[37] Yong, R.N., Youssef, A.F. and El-Mamlouk, H. "Soil Deformation and Slip Relative to Grouser Shape and Spacing". Journal of Terramechanics. 15 (3)(1978).

[38] Yong R.N. , El-Mamlouk, H. and Della-More Ha, L. "Evaluation and Predicted of Energy Losses in Terrain-Track Interaction" Journal of Terramechanics. 17 (2)(1980)

[39] Salokhe, V.M., and Gee-Clough, D. "Modes of Wet Clay Soil Behaviour Under a Single Cage Wheel Lug". Journal of Terramechanics. 25 (4)(1988)

[40] Salokhe, V.M., Rajaram, G. and Gee-Clough, D. "Limitations of Passive Earth Pressure Theory For Gage Wheel Lug and Tine Force Predictions". Journal of Terramechanics. 26(8)(1989).

[41] Kogure, K., Ohira, Y., and Yamaguchi, H. " A Simplified Method for the Estimation of Soil Thrust Exerted By a Tracked Vehicle". Journal of Terramechanics. 19 (3)(1982)

[42] Esin, A., Properties of Materials for Mechanical Design. Middle East Technical University. Ankara,(1981).

[43] _____ , Designing With High-Strength Steel Castings. Climax Molybdenum Company. New York.

[44] Shigley, J. Mechanical Engineering Design. Mc Graw Hill Book Company.(1986).

[45] Orlov, P. Fundamentals of Machine Design. Vol 3, Mir Publishers Moscow.(1986).

[46] Harzadın, T. "Türkiye'de Üretilen Traktörlerin Teknik Sorunları". Endüstri Mühendisliği Dergisi. İkinci Otomotiv ve Yan Sanayi Sempozyumu. (1. Özel Sayısı) .

APPENDICES

APPENDIX A

THE PREDICTION OF THE DRAWBAR PULL CONTRIBUTION FROM IRON-WHEEL LUGS

In chapter six it was stated that the drawbar pull contribution by the Iron-Wheel lugs will be predicted for two cases. These cases are:

Case 1 : For the Iron-Wheel with the leading lug's angle $\lambda_1 = \lambda_f$

Case 2 : For the Iron-Wheel with the leading lug's angle

$\lambda_1 = \lambda_f + \in /_2$

Since the methodology for predicting the Iron-Wheel lug's drawbar pull contribution is same for the Iron-Wheel with any leading lug angle, only a detailed methodology for prediction of the drawbar pull contribution for the Iron-Wheel at position represented by case 1 will be given. For the Iron-Wheel at position represented by case 2, only the results will be tabulated.

Case 1. ($\lambda_1 = \lambda_f$ = 1.113 radian).

Calculation of the remaining lug's angles.

Once the Iron-Wheel's leading lug's angle, λ_f is known, all the remaining lug's angles can be calculated by using equation (6.15) given below

$$\lambda_i = \lambda_1 = \lambda_f + \epsilon\,(i - 1) \quad \text{(radian)} \qquad (6.15)$$

where

$$\epsilon = \frac{2\pi}{N_i} = \text{radians} \qquad (A.1)$$

where i is the number as shown in Figure 6.1 given below.

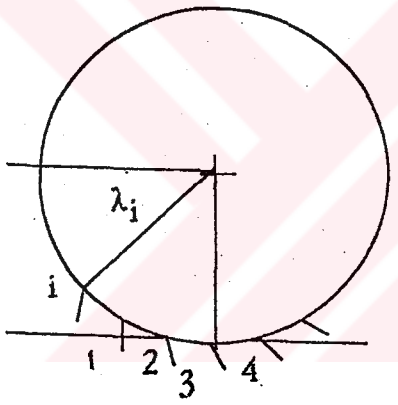

Figure 6.1 Schematic Diagram of the Iron-Wheel.

Calculation of the Soil-lug Interaction Angles.

These angles are important as they are needed for reading the Reece's factors (see chapter five) for each lug from charts given in Ref [29]. The soil-lug interaction angle for each lug can be found by using the equation below.

Calculation of Lug's Sinkage

The lug's sinkage is required for the calculation of load required at the soil-lug interface to cause soil failure for each lug and it is given as

$$Z_i = r_2 \sin \lambda_i - r_2 \sin \lambda_f - Z_{in} \quad (mm)$$

Calculation of Lug's Lateral Displacement

This is the lug's lateral displacement from the lug's first contact point, this is required for modelling the soil compressibility and it is calculated by using the equation below

$$l_i = \frac{1}{2}\left[(r_1 \cos(\lambda_f - \phi_i) + r_2 \cos \lambda_f) - (2r_1(\lambda_i - \lambda_f)(1-s) + r_2 \cos \lambda_i + r_1 \cos(\lambda_i - \phi_i)\right]$$

Calculation of Soil Compressibility Correction Factor

The equations for calculating the soil compressibility factor were derived in chapetr fiven and are given below as

$$\text{For} \begin{cases} 0 < l_i < 0.7 & P_i = 1.428\, l_i \\ l_i > 0.7 & P_i = 1 \end{cases}$$

where

$$l_i = l_i / Z_i$$

l_i : lug's lateral displacement

Z_i : lug's sinkage

The results found by using the equations above are summarized in form of Table A.1.1 below.

Table A.1.1 Values for various Parameters for Case 1

Lug Number i	Lug angles λ_i (radians)	Lug-Soil interaction angles α_i	Lug's Sinkage Z_i (mm)	Lug's lateral displacement l_i (mm)	l_i	Compressibility correction factor P_i
Lug 1	1.113	1.505	0	0	-	-
Lug 2	1.375	1.243	36.36	36.36	0.400	0.571
Lug 3	1.637	0.981	44.02	44.02	0.808	1.000
Lug 4	1.899	0.719	20.94	20.94	2.650	1.000

Reece's factors and Surcharge Pressure.

The Reece's factors for each lug are obtained from charts given in Ref [29]. by entering the soil-lug interaction angle at the appropriate chart and the soil internal friction angle. Detail information on how to use the charts can be found in Ref [29]. The Reece's factors for the lugs were obtained from the charts and are summarized in form of Table A.1.2 given below

The surcharge pressure due to the tractor weight acting on the Iron-Wheel can be found by using the equation below

$$q_i = Q / A_{un} \qquad (A.2)$$

where

Q : lug's lateral displacement

A_{un} : Iron-Wheel's surface area in contact with the soil, m^2

($A_{un} = 0.021\ m^2$)

$$q_i = 114 \text{ kPa} \qquad (A.3)$$

Due to the small soil-Iron-Wheels contact length (L = 0.07 m), the surcharge pressure can only act on soil in front of one lug. On the other lugs the effect of surcharge pressure on the load required to cause soil failure at the soil-lug interface is zero. The surcharge pressure acting on the soil infont of each lug is shown in Table A.1.2.

Table A.1.2. Reece's Factors and Surcharge Pressure of Iron-Wheel Lugs for Case 1.

Lug number i	Lug-Soil interaction angles α_i	Gravitional effect factor N_{yi}	Soil Cohession effect factor N_{ci}	Soil Adhession effect factor N_{ai}	Surcharge pressure effect factor N_{qi}	Surcharge pressure (kPa)
Lug 1	1.505	0.82	2.77	0.51	1.53	0
Lug 2	1.243	0.74	2.33	0.52	1.66	0
Lug 3	0.981	0.84	1.83	0.35	1.66	114
Lug 4	0.719	0.92	1.73	0.09	1.80	0

Calculation of the drawbar pull contribution by Iron-Wheel lugs.

The contribution of the drawbar pull by Iron-Wheel lugs will be predicted by using the equations given below.

$$T_i = \sum_{i=1}^{N_2} P_i b_i \sin(\lambda_i+\beta-\delta) - Ca\, Z_i \cos^2(\lambda_i+\beta)] \qquad (5.1)$$

where

$$L_i = YZ_i^2 N_{yi} + C_c\, N_{yi}\, Z_i + Ca\, Z_i\, N_{ai} + q_i\, Z_i\, N_{qi}$$

For the sake of simplicity equation (5.1) can be written as

$$T_i = \sum_{i=1}^{N_2} b_i L_{Hi}$$

where

$$L_{Hi} = P_i L_i \sin(\lambda_i + \beta - \delta) - Ca\, Z_i \cos^2(\lambda_i + \beta)$$

Since all the parameters required to have L_i and L_{Hi} calculated had already been found, L_i and L_{Hi} where easily calculated and their values were found for each bug as summarized in Table A.1.3

Table A.1.3. The Values for L_i and L_{Hi} for each Lug for Case 1.

Lug Number i	Lug angles λ_i (radians)	L_i (kN/m)	L_{Hi} (kN/m)
Lug 1	1.113	0	0
Lug 2	1.375	4.93	2.48
Lug 3	1.637	12.82	10.64
Lug 4	1.899	2.24	0.80

The drawbar pull contribution by Iron-Wheel lugs for case 1 is then given as

$$T_i = \sum_{1}^{4} b_i L_{Hi} = 4.18 \text{ kN} \qquad (A.4)$$

Case 2. ($\lambda_1 = \lambda_f + \in /_2 = 1.244$).

Table A.1.4. Values for Various parameter for case 2.

Lug Number i	Lug angles λ_i (radians)	Lug-Soil interaction angles α_i	Lug's Sinkage Z_i (mm)	Lug's lateral displacement l_i (mm)	l_i	Compressibility correction factor P_i
Lug 1	1.244	1.374	21.09	6.00	0.284	0.406
Lug 2	1.506	1.112	44.05	24.74	0.562	0.803
Lug 3	1.768	0.850	36.27	46.15	1.273	1.000
Lug 4	2.029	0.588	-	-	-	-

Table A.1.5 Reece's Factors and Surcharge Pressure of Iron-Wheel Lugs for Case 2.

Lug number i	Lug-Soil interaction angles α_i	Gravitional effect factor N_{yi}	Soil Cohession effect factor N_{ci}	Soil Adhession effect factor N_{ai}	Surcharge pressure effect factor N_{qi}	Surcharge pressure (kPa)
Lug 1	1374	0.78	2.33	0.50	1.60	0
Lug 2	1.112	0.78	2.00	0.46	1.60	114
Lug 3	0.850	0.84	1.60	0.20	1.73	0
Lug 4	0.588	-	-	-	-	-

Table A.1.6. The Values for L_i and L_{Hi} for each Lug for Case 2.

Lug Number i	Lug angles λ_i (radians)	L_i (kN/m)	L_{Hi} (kN/m)
Lug 1	1.244	2.806	1.08
Lug 2	1.506	13.204	9.47
Lug 3	1.768	2.908	0.96
Lug 4	2.029	-	-

The drawbar pull contribution by Iron-Wheel Lugs for Case 2 is then given as

$$T_i = \sum_{i=1}^{4} b_i L_{Hi} = 3.45 \text{ kN} \qquad (A.5)$$

The average pull contribution by the Iron-Wheel is the given by avarage of the draw bar pull contribution by the Iron-Wheel lugs for case 1 and 2 and it is found as

$$T_i = \frac{3.45 + 4.18}{2} \text{ kN}$$

$$T_i = 3.82 \text{ kN}.$$

APPENDIX B

PREDICTION OF FUNCTIONAL PERFORMANCE OF BAŞAK-17 HAVING PNEUMATIC TYRES

The functional Performance of Başak-17 having pneumatic tyres is predicted by using the tyres mobility number method introduced in chapter two. The Data necessary for the prediction of the functional performance are derived from tables in chapter four are given in Table A.2.1.

Table A.2.1 Necessary Data for Prediction of Tractor's Functional Performance.

Parameter	Value
Weight acting on each tractor rear tyre, W_r (KN)	2.4
Weight acting on each tractor rear tyre, W_f (KN)	1.12
Rear tyre diameter, d_r (m)	0.814
Rear tyre width, b_r (m)	0.209
Front tyre diameter, d_f (m)	0.508
Front tyre width, b_f (m)	0.120
Soil cone index value, C (kPa)	1500
Assumed rear wheel slip, s	0.15
Assumed value for δ_r/h_r and δ_δ/h_δ [7]	0.2

(a) Calculation of rear and front tyre mobility numbers.

The tyre mobility number will be calculated by using equation (2.11) given below

$$M_T = \frac{C\,b\,d}{W_T}\sqrt{\delta/h}\left(\frac{1}{1+b/2d}\right) \qquad (2.11)$$

The mobility number for tractor rear tyre, M_{Tr} is then calculated as

$$M_{Tr} = \frac{C\,b_r\,d_r}{W_r}\sqrt{\delta_r/h_r}\left(\frac{1}{1+b/2d}\right) \qquad (A.2.1)$$

The mobility number for tractor front, tyre, M_{Tf} is given as

$$M_{Tf} = \frac{C\,b_f\,d_f}{W_f}\sqrt{\delta_f/h_f}\left(\frac{1}{1+b_f/2d_f}\right) \qquad (A.2.2)$$

(b) Calculation of coefficient of traction for the rear tyres.

First the maximum coefficient of traction will be calculated by using equation (2.13), which is rewritten as

$$C_{mr} = 0.796 - 0.92/M_{Tr} \qquad (A.2.3)$$

The rate constant Kr will be found by using equation (2.14) which is rewritten as given below

$$K_{mr} \cdot C_{mr} = 4.838 + 0.06\,M_{Tr} \qquad (A.2.4)$$

The coefficient of traction, CTr will then be found be by using equation (2.12) rewritten as given by equation (A.2.5)

$$C_{Tr} \cdot C_{mr} = (1 - e^{-Krs}) \qquad \text{(A.2.5)}$$

(c) Calculation of coefficient of rolling resistance for the rear and front tyres.

The coefficient of rolling resistance for the tractor rear and front tyres can be found by using equation (2.15), which is rewritten as given by equations (A.2.6 and A.2.7)

$$C_{Rr} = 0.054 + 0.323/M_{Tr} \qquad \text{(A.2.3)}$$

$$C_{Rf} = 0.054 + 0.323/M_{Tf} \qquad \text{(A.2.3)}$$

(d) Calculation of Başak-17 tractor's drawbar pull and tractive efficiency

Once the coefficient of traction for the tractor rear tyres and the coefficient of rolling resistance for all the tractor tyres are determined, the tractors drawbar pull and tractive efficiency can be easily calculated by using the equations below.

$$D - \sum_{i=1}^{2} W_r C_{Tr} - D - \sum_{i=1}^{2} W_r C_{Rr} - D - \sum_{i=1}^{2} W_w C_{Rf} \qquad \text{(A.2.8)}$$

$$\eta_d = \frac{D(1-s)}{D + \sum_{i=1}^{2} W_r C_{Rr} + \sum_{i=1}^{2} W_f C_{Rf}} \times 100 \qquad \text{(A.2.9)}$$

The results obtained by using equations (A.2.1-A.2.9) are tabulated in a summary form in Table A.2.2 below.

Table A.2.2 Result Obtained through Using the Mobility Number Method

Parameter	Value
Rear tyre's mobility number, M_{Tr}	43.95
Front tyre's mobility number, M_{Tf}	32.66
Coefficient of traction for rear tyres, C_{Tr}	0.594
Maximum coefficient of traction for rear tyres, C_{mr}	0.775
Rate constant, K_r	9.700
Coefficient of rolling resistance for rear tyres, C_{Rr}.	0.061
Coefficient of rolling resistance for front tyres C_{Rf}	0.063
Tractor's drawbar pull, D (KN)	2.414
Tractor's tractive efficiency, η_d (%)	72.0

APPENDIX C

IRON-WHEEL'S MECHANICAL DESIGN

A.3.1 Introduction

It was decided in chapter six that the Iron-Wheel will consist of an aluminium rim and alloy steel shoes containing the lugs. In this appendix the design calculations will be given, but before that forces used in the design calculation are given in Table A.3.1. This Appendix should be studied while referring to the Iron-Wheels technical drawings.

Table A.3.1. Forces Experienced by the Iron-Wheel.

Force	Value
Drawbar pull (using safety factor, $N_s = 2$), KN	10
Tractor weight acting on Iron-Wheel (Using safety factor, $N_s = 2$), KN	4.8

A.3.2. Design Calculations.

(a) Iron-Wheel rim design.

(i) Tractor axle studs-Iron-Wheel studs hold.

Due to the tractor's high gear reduction ratio, the forces experienced by the Iron-Wheel's studs holds are great. This has made it necessary to weld a steel reinforcement plate on the Iron-Wheel. The material data for this plate is given in Table A.3.2. below.

Table A.3.2 Material data for the steel reinforcement plate [45].

Parameter	Value/Type
Material : steel	AISI 1020
Yield strength, N/mm^2	296
process method	Annealed

Six studs will be connecting the the Iron-Wheel to the tractor axle, the forces experienced by each said and Iron-Wheel stud hold is given as

$$\text{Force experienced by each stud} = \frac{10 \times 0.408}{0.075 \times 6} \times 1000 = 9067 \text{ N}$$

Bearing stress on Iron-Wheel stud hold $= \frac{\text{Force acting on stud}}{\text{Bearing area}} = \frac{9067}{100}$

$= 90.67 \text{ N/mm}^2$

Checking for weld's strength

Reinforcing plate's thickness = 10 mm.

Plate's external diameter = 35 mm.

Plate's external diameter = 65 mm.

The weld's strength = 34N/mm^2

Weld's external length = $2\pi \times 65 = 408.41$ mm.

Weld's enternal length = $2\pi \times 35$ 219.91 mm

Weld's width = $0.7072 \times 10 = 7.072$ mm

Weld's external shear area $408.41 \times 7.072 = 2888.28 \text{ mm}^2$

Welds internal shear area = $219.91 \times 7.072 = 1555.20 \text{ mm}^2$

Weld's stress concentration factor = 1.42

The torque the weld can stand $= \frac{34}{1.42} \times 2888.28 \times 0.065$

$+ \frac{34}{1.42} \times 1555.2 \times 0.035$

$= 5798.44$ N-m

Maximum Iron-Wheel torque = 4080 N-m, therefore the design is safe.

(ii) Iron-Wheel rib.

Material data for Iron-Wheel rib is given in Table A.3.3. In the

design calculation each rib will be considered as a cantilever beam, the maximum moment acting on each rib is given as

$$\text{Moment acting on each rib} = \frac{10 \times 1000 \times 0.25}{6} = 416.67 \text{ N.m.}$$

Table A.3.3. Material data for the Iron-Wheel ribs and bolt hold connecting to Iron-Wheel shoes.

Parameter	Value/Type
Material : Aluminium alloy	LM5-M
Yield strength, N/mm^2	100
Fatique strength, N/mm^2	95
Fatique strength modifying factors:	
Size factor	0.80
Surface quality factor	0.80
Stress concentration factor	1.80
Part's fatique strength, N/mm^2	60.8

$$\text{The maximum rib width} = \sqrt{\frac{416.67 \times 10\ 12 \times 1.8}{2 \times 6 \times 60.8}} = 111.1 \text{mm.}$$

The rib width in the design is move than 111.1 mm, Therefore the design is safe.

(iii) Iron-Wheel rim bolt hold connecting to Iron-Wheel shoes.

The material data for Iron-Wheel rim bolt hold connecting to Iron-Wheel shoes is given in Table A.3.3. Force acting on each Iron-Wheel shoes bolt is given as

Force acting on each bolt $= \frac{10 \times 10^3}{4} = 2500N.$

Bearing stress $= \frac{1.8 \times 2500}{220} = 20.45 < 60.8 N/mm^2.$

The design is safe.

(b) Iron-Wheel shoe design

(i) Design Calculation for Iron-Wheel lugs.

The most critical part of Iron-Wheel shoes is the lugs. The lugs are loaded by bending moments in two form as given below.

Bending moment due to the drawbar pull

=22.5x10000=225000 N-mm.

Bending moment due to tractor weight

= 26.0 x 4800 = 124800 N-mm.

Since the two bending moments do not act on the lug as the same time; the calculation will be done by using the greater bending moment. The material data for the Iron-Wheel shoe is given in Table A.3.4.

Table A.3.4. Material data for the Iron-Wheel shoes.

Parameter	Value/Type
Material : Steel (N_i, C_r, M_o)	AISI 4340
Tensile strength, N/mm^2	965
Fatigue strength, N/mm^2	489
Fatigue strength modifying factor:	
Size factor	0.7
Surface quality modifying factor	0.5
Stress concentration factor	1.8
Part's fatigue strength, N/mm^2	171.15

Lug's thickness - 7 mm.

$$I = \frac{1}{12} bh^3 = \frac{1}{12} \times 300 \times (7)^3 = 8575 \text{ mm}^4$$

$$\text{Bending stress} = \frac{1.8 \times 225000 \times 3.5}{8575} = 165.3 \text{ N/mm}^2$$

The bending stress = 165.30 < 171.15 therefore the design is safe.

(c) Iron-Wheel's approximate weight

Since the heaviest part of the Iron-Wheel is the Iron-Wheel shoes and it's weight will be calculated first as shown below.

Approximate volume of Iron-Wheel shoes $= \pi(40.6^2 - 40^2).30 +$

$0.7 \times 30 \times 24$

$= 5061.82\ cm^3$

Approximate weight of Iron-Wheel shoes $= \frac{5061.82 \times 7.68}{1000} = 38.87$ Kg.

The Iron-Wheel rim's weight is found as shown below

Approximate volume of Iron-Wheel rim $= \pi(34^2 - 3.5^2) \times 0.6$

$+ \pi(40^2 - 39.6^2) \times 30$

$= 6645.48\ cm^3$

Approximate weight of Iron-Wheel rim $= \frac{6645.88 \times 2.7}{1000} = 17.94$ Kg.

Total weight of Iron-Wheel $\cong 57.42$ Kg

An all steel Iron-Wheel weight = 90.00 Kg, this is clearly not portable.